



Universiteit
Leiden
The Netherlands

Immunological aspects of conventional and new treatments for cervical cancer, an immunopharmacological approach

Meir, H. van

Citation

Meir, H. van. (2017, April 12). *Immunological aspects of conventional and new treatments for cervical cancer, an immunopharmacological approach*. Retrieved from <https://hdl.handle.net/1887/48288>

Version: Not Applicable (or Unknown)

License: [Licence agreement concerning inclusion of doctoral thesis in the Institutional Repository of the University of Leiden](#)

Downloaded from: <https://hdl.handle.net/1887/48288>

Note: To cite this publication please use the final published version (if applicable).

Cover Page



Universiteit Leiden

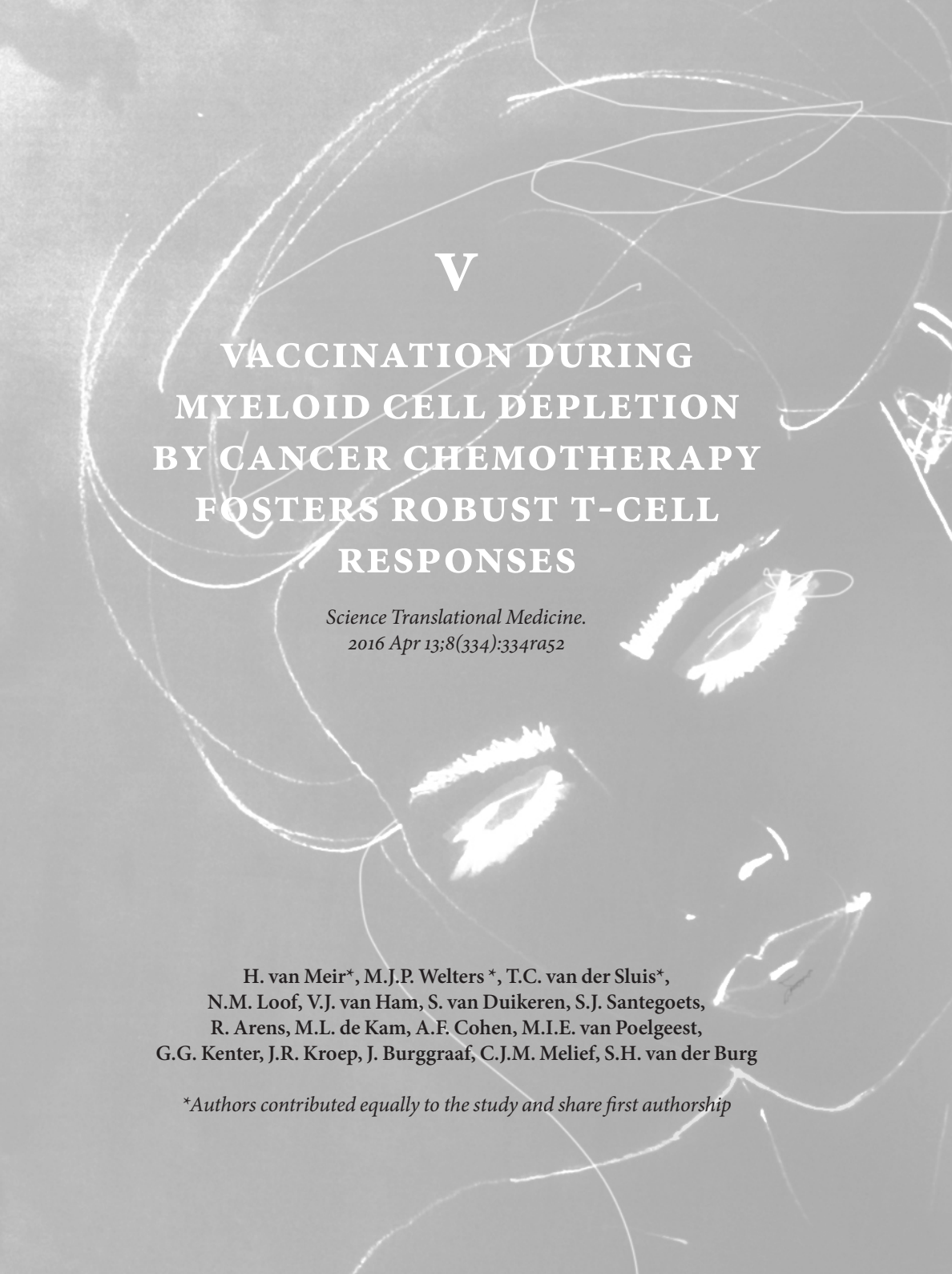


The handle <http://hdl.handle.net/1887/48288> holds various files of this Leiden University dissertation

Author: Meir, H. van

Title: Immunological aspects of conventional and new treatments for cervical cancer, an immunopharmacological approach

Issue Date: 2017-04-12



V
VACCINATION DURING
MYELOID CELL DEPLETION
BY CANCER CHEMOTHERAPY
FOSTERS ROBUST T-CELL
RESPONSES

Science Translational Medicine.
2016 Apr 13;8(334):334ra52

H. van Meir*, M.J.P. Welters*, T.C. van der Sluis*,
N.M. Loof, V.J. van Ham, S. van Duikeren, S.J. Santegoets,
R. Arens, M.L. de Kam, A.F. Cohen, M.I.E. van Poelgeest,
G.G. Kenter, J.R. Kroep, J. Burggraaf, C.J.M. Melief, S.H. van der Burg

**Authors contributed equally to the study and share first authorship*

ABSTRACT

Therapeutic vaccination with human papillomavirus type 16 synthetic long peptides (HPV16-SLPs) results in T-cell-mediated regression of HPV16-induced premalignant lesions but fails to install clinically effective immunity in patients with HPV16-positive cervical cancer. We explored whether HPV16-SLP vaccination can be combined with standard carboplatin and paclitaxel chemotherapy to improve immunity and which time point would be optimal for vaccination. This was studied in the HPV16 E6/E7-positive TC-1 mouse tumor model and in patients with advanced cervical cancer. In mice and patients, the presence of a progressing tumor was associated with abnormal frequencies of circulating myeloid cells. Treatment of TC-1-bearing mice with chemotherapy and therapeutic vaccination resulted in superior survival and was directly related to a chemotherapy mediated altered composition of the myeloid cell population in the blood and tumor. Chemotherapy had no effect on tumor-specific T-cell responses. In advanced cervical cancer patients, carboplatin-paclitaxel also normalized the abnormal numbers of circulating myeloid cells, and this was associated with increased T-cell reactivity to recall antigens. The effect was most pronounced starting 2 weeks after the second cycle of chemotherapy, providing an optimal immunological window for vaccination. This was validated with a single dose of HPV16-SLP vaccine given in this time window. The resulting proliferative HPV16-specific T-cell responses were unusually strong and were retained after all cycles of chemotherapy. In conclusion, carboplatin-paclitaxel therapy fosters vigorous vaccine induced T-cell responses when vaccination is given after chemotherapy and has reset the tumor-induced abnormal myeloid cell composition to normal values.

Introduction

The majority of cervical cancers is induced by human papillomavirus type 16 (HPV16).¹ Up to 70% of the advanced cancers relapse.²⁻³ One of the preferred treatments for patients with recurrent, metastatic, or advanced cervical carcinoma is the combination of carboplatin with paclitaxel (CarboTaxol)⁴, but this is rarely curative.⁵

The two HPV16-encoded oncoproteins E6 and E7 are required for the transformation of epithelial cells⁶ and constitute excellent targets for the immune system. HPV16-specific T-cell reactivity is frequently detected in healthy individuals but usually not in patients with premalignant anogenital lesions or cancer.⁷ Installment of robust HPV16-specific immunity by vaccination with therapeutic HPV16 overlapping synthetic long peptides (HPV16-SLPs) admixed with Montanide ISA-51 resulted in regressions of HPV16-induced premalignant lesions of the vulva in two independent studies.⁸⁻¹⁰ In contrast, therapeutic vaccination of patients with advanced or recurrent HPV16-positive cervical cancer partly installed HPV16-specific T-cell reactivity, particularly in patients with a less suppressed immune status, but had no clinical effect.¹¹

Chemotherapeutic agents act on cancer cells¹², but many of them mediate part of their therapeutic effects through immune mechanisms.^{13,14} In murine models, the combination of chemotherapy with activation of T-cells resulted in improved treatment of tumors.¹³⁻¹⁶ Therefore, we investigated whether CarboTaxol could be successfully combined with HPV16-SLP vaccination, first in a mouse model¹³ and then in an open label observational study with cervical cancer patients.

Materials and Methods

STUDY DESIGN

The aim of the study was to test whether CarboTaxol could be combined with HPV16-SLP vaccination. We first used the HPV16 E6/E7-expressing TC-1 tumor mouse model to define the impact of CarboTaxol on systemic and intratumoral immunological parameters as well as on the clinical efficacy of vaccination. After observing that CarboTaxol did not affect lymphocytes but had a strong effect on myeloid cells and improved tumor control by therapeutic vaccination, we started a multi-center, open label, observational study, entitled 'Immunological aspects of combined chemo-immunotherapy in patients with advanced cervical cancer' (EudraCT 2010-018841-76), consisting of two cohorts of patients. In

the first cohort, 6 patients with advanced, recurrent, or metastatic cancer were treated with 6 cycles of CarboTaxol every 3 weeks, and the composition and function of the myeloid and lymphoid cells in peripheral blood were analyzed. After identifying a specific time window during chemotherapy potentially permitting the best T-cell response, we studied the second cohort of patients. In this cohort, 12 patients were treated with CarboTaxol and one dose of an HPV16 SLP vaccine 2 weeks after the second cycle of CarboTaxol. Blood samples were drawn to validate the observations made in the first cohort as well as to study the vaccine-induced T-cell response. The investigators performing and analyzing immunological assays were blinded to the clinical parameters of the patients. The data from the immunomonitoring studies are reported according to the recommended standard format 'minimal information about T-cell assays.'

MICE AND TUMOR TREATMENT

Female C57BL/6 mice (6 to 8 weeks old; Charles River Laboratories) were housed in individually ventilated cage systems under specific pathogen-free conditions. The experiments were approved by the Animal Experiments Committee of Leiden University Medical Center (LUMC), in line with the guidelines of the European Committee. The tumor cell line TC-1 is of C57BL/6 origin and expresses HPV16 E6 and E7.¹⁷ TC-1 tested negative for rodent viruses by polymerase chain reaction. Mice were subcutaneously inoculated with 1×10^5 TC-1 tumor cells. When a palpable tumor was present on day 8, mice were split into groups with comparable tumor size and treated with carboplatin [40 mg/kg, day 8, intraperitoneally], paclitaxel (20 mg/kg, days 8 and 9, intraperitoneally), and/or subcutaneous synthetic long HPV16 E743-77 peptide (SLP; GQAEPDRAHYNIVTFCCKDSTLRRCVQSTHVDIR; 150 µg) dissolved in dimethyl sulfoxide (Sigma), diluted in phosphatebuffered saline (B. Braun), and emulsified in Montanide ISA-51 (Seppic). Chemotherapy was repeated 1 week later (day 15 for carboplatin and days 15 and 16 for paclitaxel), and vaccination was repeated 2 weeks after initial treatment (day 22). Detailed information on the immunomonitoring and statistics is given in the Supplementary Materials.

PATIENTS

Patients with clinical and radiological evidence of advanced-stage, recurrent, or metastatic cervical cancer; with no curative treatment options; and scheduled for CarboTaxol were enrolled between January 2011 and January 2013. Other

inclusion criteria were as follows: (I) mentally competent patients 18 years or older, (II) no other active malignancy, (III) no indication of active infectious disease such as HIV, (IV) and no other condition that may jeopardize the health status of the patient. Patients were followed until 2 to 3 weeks after they had received their last chemotherapy cycle and thereafter at standard visits. LUMC, Academic Medical Center (Amsterdam), Free University Medical Center (Amsterdam), and Netherlands Cancer Institute–Antoni van Leeuwenhoek Hospital (Amsterdam) were the participating hospitals.

HPV typing was performed on the tumor and/or smears taken at study entry⁸, but it was not part of the inclusion criteria. The study was conducted in accordance with the Declaration of Helsinki (October 2008) and approved by the Central Committee on Research Involving Human Subjects (NL31572.000.10) in agreement with the Dutch law for medical research involving humans.

TREATMENT OF PATIENTS

For the first cohort, six of the nine screened and eligible patients participated and were treated at their hospital with CarboTaxol, consisting of carboplatin (dose based on renal function; area under the curve of six regimen) and paclitaxel (175 mg/kg²) on day 1 of each cycle, every 3 weeks for a maximum of six cycles. The patients were subjected to serial blood sampling. According to the oncology protocols, routine premedication consisting of dexamethasone [20 mg, intravenously (iv)], ranitidine (50 mg in 100 ml of NaCl 0.9%, iv), granisetron (1 mg in 100 ml of NaCl 0.9%, iv), and clemastine (2 mg in 100 ml of NaCl 0.9%, iv) was administered immediately before chemotherapeutic treatment. In case of severe hematological toxicity, neurotoxicity, nephrotoxicity, or gastrointestinal toxicity, dose modifications of carboplatin and paclitaxel were made according to the following standard scheme: (i) if the absolute neutrophil count was $< 1.5 \times 10^9$ /liter, platelet count was $< 100 \times 10^9$ /liter, or other toxicities were higher than grade 2, then CarboTaxol treatment was postponed for at least a week (or longer until the patients had recovered), and the doses of both chemotherapeutic compounds were reduced by 25%; (ii) if the patient experienced neuropathy higher than grade 2, paclitaxel was stopped but carboplatin was continued. After the completion of immunomonitoring of these first 6 patients, a second group of 12 patients (cohort 2) received CarboTaxol at their hospital at the same schedule and dose, as well as a single subcutaneous vaccination of the HPV16-SLP vaccine (300 µg per peptide emulsified in Montanide ISA-51) consisting of two mixes of peptides injected separately in the left and right limb (either arm or leg)⁹ at

LUMC, 2 weeks after the second cycle of CarboTaxol. For cohort 2, 18 advanced cervical cancer patients were screened, 5 patients declined participation, and 1 patient (ID6002) died of her disease before receiving the vaccine.

CLINICAL EVALUATION OF SAFETY AND TOLERABILITY

The safety and toxicity of treatment were evaluated according to the National Cancer Institute CTCAE v3.0. Well-known toxicities of CarboTaxol were classified as study-related events. Before the start of CarboTaxol and before vaccination, patients were physically examined and medical history was obtained. Vital signs were measured, and the injection site was inspected 15 min, 1 hour, and 4 hours after vaccination. Patients were followed with routine visits (every 3 months until progression) to monitor for AEs. For each vaccine-related AE, the relationship to HPV16-SLP was defined as definite, probable, or possible. Injection site reactions were classified as definitely vaccine-related. Injection site reaction grade 1 was defined as swelling, erythema, and tenderness (pain/itching). Injection site reaction grade 2 was defined as tenderness or swelling with inflammation or phlebitis. Injection site reaction grade 3 was defined as severe ulceration or necrosis. Venous blood samples were drawn for routine hematological analysis, including leukocyte differential counts and biochemistry assessments. Patients were followed up until date of death or loss to follow-up.

IMMUNOMONITORING OF CLINICAL TRIAL

Blood samples from patients were taken at the time points indicated in figure 4A. In addition, 19 healthy volunteers donated blood. PBMCs were isolated by Ficoll gradient centrifugation, and cells were subjected to LST.⁹⁻¹¹ MRM and influenza peptide pools served as positive controls. The remaining cells were cryopreserved until use. Thawed PBMCs were tested for their response to PHA in a proliferation assay^{18,19}, for their antigen-presenting capacity in an MLR¹⁹, and for their HPV16-specific T-cell responses by intracellular cytokine staining.¹⁰ The 11-day stimulated nondepleted and CD14-depleted PBMC samples were analyzed by a proliferation assay for antigen recognition.²⁰ The supernatants of the proliferation assays were used for cytokine analysis by cytometric bead array.⁹⁻¹¹ Immunophenotyping of the PBMC samples was performed by flow cytometry.¹⁹ Detailed information on immunomonitoring and statistics is given in the Supplementary Materials.

Results

COMBINED CHEMOIMMUNOTHERAPY IMPROVES THE ERADICATION OF HPV16-POSITIVE TUMORS IN MICE

To test the effects of CarboTaxol with HPV16-SLP vaccination, HPV16 E6- and E7-positive TC-1 tumor bearing mice were treated when tumors were palpable at day 8 (~4 mm², figure 1A). CarboTaxol had little effect on tumor growth, whereas vaccination induced a temporary decrease in tumor size (figures 1B and 1C). The combined treatment had the strongest antitumor effect (figures 1B and 1C). None of the treatments affected the percentages of circulating CD8⁺ and CD4⁺ T-cells (figures 1D and 1E; figures S1A and S1B). Vaccination induced HPV16-specific CD8⁺ T-cells, and this was not influenced by co-treatment with CarboTaxol (figure 1F and figure S1C).

CARBOTAXOL TREATMENT ALTERS CIRCULATING AND INTRA-TUMORAL MYELOID CELL POPULATIONS

To understand the mechanism underlying these improved therapeutic outcomes, immune cells in blood and tumors were analyzed 3 to 4 days after CarboTaxol treatment (and/or 9 to 10 days after peptide vaccination) (figure 2A), which is at the start of the tumor regression phase (figure S2). In untreated tumor-bearing mice, the percentage of circulating myeloid cells increased (figure S3A) because of the increase in circulating CD11b^{hi} cells, in particular, CD11b^{hi}Gr-1^{hi} cells. However, their numbers decreased markedly in tumor-bearing animals treated with CarboTaxol (figures 2B and 2C, and figure S3). The frequencies of CD4⁺ and CD8⁺ T-cells, antigen-specific CD8⁺ T-cells, monocytes, and dendritic cells in the blood were not affected by CarboTaxol treatment (figure S3). Thus, CarboTaxol treatment normalized the myeloid cell populations in the blood of tumor-bearing mice, making them more similar to those of naïve mice. This effect could not be ascribed to one individual chemotherapeutic compound because the effect on circulating CD11b^{hi} cells was particularly pronounced in animals treated with both compounds (figure S4).

Next, we assessed the effects of CarboTaxol-vaccine combination treatment on the tumor microenvironment.¹⁴ The percentage of intra-tumoral leukocytes increased upon treatment with CarboTaxol and/or vaccine (figure 2D). In vaccinated mice, a markedly high percentage of these leukocytes were CD8⁺ T-cells (figure 2E), half of which were vaccine-specific (figure 2F) and capable of

producing IFN- γ and TNF α (figure 2G). There was no direct effect of CarboTaxol treatment on the presence and function of these lymphocytes. We then focused on the intra-tumoral CD11b^{hi} myeloid cells because the Gr-1^{hi} subtype of this cell population was increased in the blood of untreated tumor-bearing mice. The Gr-1^{hi} cells in the tumors strongly expressed the granulocytic marker Ly6G and decreased amounts of the macrophage marker F4/80 and the dendritic cell marker CD11c. In contrast, Gr-1^{int}-cells had a higher expression of F4/80, CD11c, CD80, CD86, and major histocompatibility complex class II, but not Ly6G (figure 3A), suggesting a superior immune stimulatory capacity. Treatment with either CarboTaxol or vaccine resulted in a predominance of the CD11b^{hi}Gr-1^{int} population over the Gr-1^{hi} population (figures 3B and 3C). Together, these data demonstrate that treatment of tumor-bearing mice with CarboTaxol results in a relative loss of myeloid cell-associated immunosuppression in both tumor and blood.

A SPECIFIC TIME WINDOW IS ASSOCIATED WITH INCREASED IMMUNITY IN PATIENTS ON CHEMOTHERAPY

On the basis of the above observations, we performed a study in patients with advanced, recurrent, or metastatic cervical carcinoma. The trial was designed to study the impact of chemotherapy on vaccine-induced immunity, and therefore patients were not required to have an HPV16 positive tumor. Patients were screened between January 2011 and January 2013 in 4 Dutch hospitals, and their characteristics are listed in table S1. In the first cohort of 6 patients, the number and function of lymphoid and myeloid cells was studied in blood samples taken at different time points during and after CarboTaxol treatment (figure 4A). CarboTaxol treatment was associated with a decrease in the otherwise high frequency of myeloid cells (median of 32% at baseline), which reached its nadir at 1 to 2 weeks after the second chemotherapy cycle (median of 6% at 1 to 2 weeks after chemo cycle 2; figures 4B and 4C) and coincided with an increase in the percentages of lymphoid cells (figure 4D). Although the relative frequencies of CD4⁺ and CD8⁺ T-cells (figure S5) remained unchanged, T-cell function was improved, as evidenced by the increase in their proliferation against a bacterial recall antigen mixture (MRM) in the same time window (figure 4E). T-cell responses to phytohemagglutinin (PHA) stimulation were strong at all time points, indicating that there were no intrinsic problems with the T-cells' response to mitogens (figure S5). The capacity of antigen presenting cells (APC) to stimulate allogeneic T-cell proliferation was slightly improved (figure 4F). Thus, the observations in mice are mirrored by the findings in patients. Furthermore,

the results revealed a specific time window throughout CarboTaxol treatment, during which antigen-specific T-cell responses were optimal. This time window, starting at 1 to 2 weeks after the second cycle of CarboTaxol, appeared attractive for the generation of strong T-cell responses by vaccination. We used this observation to select the time window for the application of a single dose of vaccine in the second patient cohort.

CARBOTAXOL MEDIATES NORMALIZATION OF CIRCULATING IMMUNE CELL FREQUENCIES

The second cohort consisted of 13 patients (table s1). One patient (ID6002) died of progressive disease before vaccination and was substituted by ID6102. Compared to 19 healthy donors, the patients from both cohorts displayed an increased frequency of circulating myeloid cells before chemotherapy (figure s6A), confirming that the progressive tumor growth-induced myeloid changes in mice are mirrored in patients with advanced cervical cancer (figure 4). Throughout the CarboTaxol treatment, the absolute numbers of lymphocytes remained similar (figure 5A), but the absolute number of circulating leukocytes was strongly reduced (median $-4.7 \times 10^9/L$) as measured by leukocyte differentiation analyses (figure 5B). This reduction reached its nadir after two cycles of chemotherapy and was retained during the remainder of the chemotherapy cycles. Flow cytometry analysis again revealed a decrease in myeloid ($CD45^+CD3^+CD19^-$) and a relative increase in lymphoid ($CD45^+CD3^+CD19^+$) cells (figures s6B and s6C). The frequency of these populations almost normalized to the levels observed in healthy donors (Figures 5C and 5D), and this correlated with an increased T-cell responsiveness to bacterial (MRM; figure 5E) and viral antigens (FLU; figure 5F). Similar to the first cohort, the blood samples of cohort 2 showed no overt changes in APC function or the response to PHA stimulation (figure s5).

Further dissection of the changes within the myeloid ($CD45^+CD3^+CD19^-CD11a^-$) cell population was performed on the basis of HLA-DR expression, to distinguish macrophages and dendritic cells (DCs; $HLA-DR^+$) from myeloid-derived suppressor cells (MDSCs; $HLA-DR^{low}$) and further subdivide them on the expression of CD14 and CD11b within the $HLA-DR^+$ myeloid cell population (figure s7). Of the five identified subpopulations, population 1 ($CD14^+CD11b^+$) and population 2 ($CD14^{int}CD11b^{int}$) were most abundant and increased before CarboTaxol treatment when compared to healthy donors (figures 6A and 6B and figure s8). The other 3 populations each constituted 0.2 to 2.6% of the myeloid cell fraction. During chemotherapy, the frequencies of populations 1, 3, and 5 dropped (figure 6B and figure s8). The treatment-induced decrease in population

1 coincided with improved T-cell reactivity against MRM and FLU (figure 6C). Extended analysis of the various subsets by flow cytometry (figure S7) revealed that population 1 was comprised of M1 monocytes/macrophages ($CD45^+CD3^-CD19^-CD1a^-HLA-DR^+CD14^+CD11b^+CD206^-CD163^-CD16^-CD11c^+$) and M2c monocytes/macrophages ($CD45^+CD3^-CD19^-CD1a^-HLA-DR^+CD14^+CD11b^+CD206^-CD163^-CD16^-CD11c^+$). The frequency of both subpopulations was increased in patients but normalized upon treatment (figures 6D and 6E). The frequency of 10 distinct circulating MDSC populations²¹ was not different between patients and healthy donors. Only the main MDSC population ($CD45^+CD3^-CD19^-CD1a^-HLA-DR^{low}$) displayed a slight decrease during chemotherapy (Figure 6F and figure S7).

Analysis of the T-cell populations (figure S7) revealed no changes in $CD4^+$ and $CD8^+$ T-cell frequencies (figures S9A and S9B), confirming our findings in mice. The frequency of TIM3 (T-cell immunoglobulin domain and mucin domain-3) and/or PD-1 (programmed cell death protein 1)-expressing $CD4^+$ or $CD8^+$ T-cells (figures S9C and S9D) and $CD4^+CD25^+CD127^-FOXP3^+$ regulatory T-cells (figure S9E) was higher in patients when compared to healthy controls. The percentage of $CD4^+TIM3^+PD1^-$ and that of regulatory T-cells slightly decreased during chemotherapy (figures S9C and S9E).

Together these results showed that CarboTaxol treatment strongly affected myeloid cells but not lymphocytes. CarboTaxol treatment normalized the amounts of different myeloid cell populations found to be increased in the blood of cervical cancer patients. This normalization of myeloid cell numbers coincided with improved T-cell reactivity to antigens from common pathogens, suggesting a relief from general immune suppression.

TIMED VACCINATION DURING CHEMOTHERAPY RESULTS IN A STRONG AND SUSTAINED HPV16-SPECIFIC T-CELL RESPONSE

Twelve patients received a single vaccination with the HPV16-SLP vaccine^{8,10,11} at 2 weeks (13 to 17 days) after the second (n = 11) or third cycle of chemotherapy (n = 1; ID6008). None of the patients had a demonstrable pre-existing response to HPV16 E6/E7. Vaccination with the HPV16-SLP vaccine induced proliferative T-cell responses in 11 patients (figure 7A). The median stimulation index to all 6 peptide pools was 25.0 (range 4.3 to 133.4) at 3 weeks after vaccination in these responders. Vaccine-induced HPV16-specific proliferation was retained after 6 cycles of chemotherapy and in some cases even increased (median 21.0; range 5.0 to 141.5; figure 7A, black versus gray bars). The vaccine-specific proliferative T-cell response in the 7 HPV16 positive patients was not statistically higher than in the other patients (figure 7B). For six patients, enough PBMCs were available

to analyze the vaccine-induced T-cell response by intracellular staining for IFN- γ , IL-2, and TNFA. A poly-functional cytokine response to HPV16 E6 was measured in five and to E7 in four out of the six patients. One patient (ID6004) was anergic (figure s10), confirming the results of the proliferation assay (figure 7A). Previously, patients with recurrent HPV16 positive cervical cancer were vaccinated at least 1 month after chemotherapy.¹¹ In comparison to the responses seen during the earlier trial, the proliferative responses obtained by vaccination during chemotherapy were of far greater magnitude (figure s11).

MYELOID CELL DEPLETION IMPROVES THE RESPONSE OF PBMC TO STIMULATION IN VITRO

To recapitulate *in vitro* the association between a reduced myeloid cell population and improved T-cell reactivity to recall antigens and HPV16 vaccination, we depleted myeloid cells from the PBMC of two patients displaying relatively high frequencies of myeloid cells before chemotherapy and stimulated these PBMC with autologous monocytes pulsed with a mix of recall antigens, a mix of E6 and E7 peptides, or a mix of p53 peptides as control for 11 days before the antigen-specific T-cell response was tested. As a control, we used non-depleted PBMC. Not only was the T-cell response to recall antigens much higher in the culture started with myeloid cell-depleted PBMC, but the HPV16-specific response was also more efficiently boosted during these 11 days. As expected, no reactivity was detected in the cultures stimulated with the control p53 peptides (figure s12).

COMBINATION OF CHEMOTHERAPY WITH VACCINATION IS SAFE IN ADVANCED CERVICAL CANCER PATIENTS

Safety was assessed according to Common Terminology Criteria for Adverse Events (CTCAE) version 3.0. Most of the observed adverse events (AEs) were disease-related or chemotherapy-related. All patients developed chemotherapy-related anemia, thrombocytopenia, leucopenia, neutropenia, and alopecia. There were seven AEs, all in different patients, related to the advanced stage of the disease: shortness of breath, pulmonary embolism, abdominal pain (lymphedema), gastroenteritis, erysipelas, hydronephrosis. One patient (ID6002) died before vaccination could take place, and one patient (ID6004) died 11 weeks after vaccination. The cause of death in both cases was progressive disease. Vaccine-related AEs were largely localized to the vaccination site (table s2). One patient developed an ulcer at the injection site, which persisted for more than 6 weeks and required antibiotic treatment.

Discussion

Here, we observed that tumors expressing the HPV16 oncoproteins E6 and E7 cause the numbers of circulating myeloid cells to be abnormally high in TC-1-challenged mice and in HPV-positive cervical cancer patients. Treatment with CarboTaxol normalizes the numbers of circulating myeloid cells but has no negative effect on the number and function of lymphocytes. In mice, CarboTaxol treatment had a similar effect on the myeloid cell composition within the tumors as in the blood. The effects of CarboTaxol are, therefore, not limited to circulating immune cells, and it is likely that similar effects occur within the tumors of cervical cancer patients. The CarboTaxol-mediated normalization of circulating myeloid cells was associated with increased T-cell-mediated tumor control in mice and with higher T-cell reactivity against common microbial recall antigens and response to HPV16-SLP vaccination in patients. This suggests a causal relationship between the normalization of abnormally high myeloid cell frequencies and improved T-cell responsiveness. Because the combination of HPV16-SLP vaccination plus CarboTaxol improved the cure rate of mice with established TC-1 tumors, we expect that the robust and sustained HPV16-specific T-cell responses seen with this combination improved the efficacy of treatment in patients with advanced cervical cancer. This needs to be studied in a future randomized clinical trial.

CarboTaxol is a standard chemotherapeutic treatment not only in cervical cancer but also in patients with other cancer types, including lung cancer and ovarian cancer. Its effect on the immune system, however, has not been widely studied. Carboplatin and paclitaxel are both known to cause dose-limiting myelotoxicity.^{22,23} This is likely a direct effect on precursor cells in the bone marrow, as observed in different animal models.²⁴ White bone marrow cells display impaired *in vitro* capacity to proliferate when treated with carboplatin.²⁵ Furthermore, the number of myeloid cells reaching its nadir at 2 weeks and a rebound at 3 weeks after CarboTaxol treatment is in line with the mechanistic models for the development and maturation of leukocytes and drug susceptibility in the bone marrow.^{26,27} Lymphopenia has not been reported. We observed an increase in T-cell reactivity 1 to 2 weeks after the second and subsequent cycles of chemotherapy. This was not a result of changes in absolute lymphocyte counts or strong alterations in the number or phenotype of CD4⁺, CD8⁺, or regulatory T-cells. Similar observations were made in ovarian cancer patients. Those patients who responded to CarboTaxol displayed a stronger IFN- γ -producing CD8⁺ T-cell response during treatment 12 to 14 days after chemotherapy.^{28,29} Here we show that the positive effect of CarboTaxol on

the immune response results from the normalization of abnormal myeloid cell numbers, which are initially high in the presence of larger tumor burden. Leukocytosis has been described in patients and animals with HPV-associated cancers^{30,31}, but the composition of the increased leukocyte populations was not analyzed in detail. An in-depth analysis of the myeloid cell subsets affected by CarboTaxol revealed that these effects were found across all subsets that are elevated in patients or in tumor-bearing animals. This includes tumor growth-suppressing myeloid cells, but more importantly the tumor-promoting myeloid cell populations which can suppress the function of anti-tumor effector T-cells. Apparently, the balance among these subsets and in particular the decline in immunosuppressive myeloid cells within the tumor microenvironment appears to be important for successful implementation of immunotherapy and improved clinical efficacy. The change in the proportions of myeloid cells and lymphocytes allowed the latter population to respond to antigenic stimulation, most likely through a relief from myeloid cell-mediated immunosuppression. This notion is sustained by the unexpectedly high proliferative responses after timed application of a single vaccination and our *in vitro* experiment showing that removal of excessive CD14⁺ myeloid cells from pre-chemotherapy PBMC samples of two cancer patients allowed the tumor-specific T-cells to react to antigenic stimulation. This seems to be a general phenomenon, and we observed this also in the context of lung cancer.²⁰ A recent phase II trial in patients with extensive small-cell lung cancer reported that ipilimumab treatment beginning with the third cycle of CarboTaxol produced better clinical outcomes than giving the drugs during cycles 1 to 4.³² The effect of CarboTaxol on myeloid cells may have relieved myeloid cell-mediated suppression of T-cells, as in our study, providing ipilimumab the opportunity to release the brakes on activated T-cells in the later phase of treatment. The effects of CarboTaxol on myeloid cells are clear in patients with cancers where myeloid cells have prognostic value^{33,34}, of which cervical and ovarian carcinomas are prime examples. Other types of cancer in which myeloid cells play an important immunosuppressive and prognostic role are thus also candidates for timed immunotherapy.

Our study has some limitations. First, although abnormal numbers of myeloid cells are found both in the mouse model and in patients, their phenotype differs. In mice, the chemotherapy-related reduction in circulating CD11b^{hi}Gr-1^{hi} cells reflected their depletion in the tumor. In patients, a number of circulating myeloid cell subsets was reduced but whether this also occurs in the tumor remains to be established. Second, in comparison to the T-cell responses obtained in our earlier studies, the current ones were of far greater magnitude. Although the tests were performed by the same laboratory according to the

same standard operating procedures, we did not perform a formal head-to-head comparison, and future trials should confirm these findings. Finally, both the strength of the vaccine-induced immune response and the reduction in circulating myeloid cells were retained for up to 2 weeks after the sixth cycle of CarboTaxol. It is not clear if stopping chemotherapy will coincide with a quick rebound of the myeloid cells, how this affects the vaccine-induced immune response, and whether the phenotype of myeloid cells will be altered under the influence of vaccine-activated T-cells. These should all be subjects of future investigations.

In conclusion, we have shown that CarboTaxol chemotherapy not only is devoid of immunosuppressive effects on tumor-specific T-cells, but vigorously stimulates tumor-specific immunity by normalizing the abnormal numbers of the immunosuppressive myeloid cell populations. Additional studies will have to demonstrate whether CarboTaxol and adequately timed HPV16-SLP vaccination also produce clinical benefit in patients with advanced cervical cancer. A larger clinical trial is already under way to test this (NCT02128126). If successful, this immunotherapeutic approach should be easy to implement because it combines smoothly with the preferred chemotherapy treatment for advanced cervical cancer.

REFERENCES

- 1 G. Y. Ho, A. S. Kadish, R. D. Burk, J. Basu, P. R. Palan, M. Mikhail, S. L. Romney, HPV 16 and cigarette smoking as risk factors for high-grade cervical intra-epithelial neoplasia. *International journal of cancer. J. Int. Cancer* 78, 281-285 (1998).
- 2 T. W. Burke, W. J. Hoskins, P. B. Heller, M. C. Shen, E. B. Weiser, R. C. Park, Clinical patterns of tumor recurrence after radical hysterectomy in stage IB cervical carcinoma. *Obstet. Gynecol.* 69, 382-385 (1987).
- 3 D. M. Larson, L. J. Copeland, C. A. Stringer, D. M. Gershenson, J. M. Malone, Jr., C. L. Edwards, Recurrent cervical carcinoma after radical hysterectomy. *Gynecol. Oncol.* 30, 381-387 (1988).
- 4 B. J. Monk, M. W. Sill, D. S. McMeekin, D. E. Cohn, L. M. Ramondetta, C. H. Boardman, J. Benda, D. Cella, Phase III trial of four cisplatin-containing doublet combinations in stage IVB, recurrent, or persistent cervical carcinoma: a Gynecologic Oncology Group study. *J. Clin. Oncol.* 27, 4649-4655 (2009).
- 5 D. Lorusso, F. Petrelli, A. Coimu, F. Raspagliesi, S. Barni, A systematic review comparing cisplatin and carboplatin plus paclitaxel-based chemotherapy for recurrent or metastatic cervical cancer. *Gynecol. Oncol.* 133, 177-123 (2014).
- 6 H. zur Hausen, Papillomaviruses and cancer: from basic studies to clinical application. *Nat. Rev. Cancer*, 342-350 (2002).
- 7 S. H. van der Burg, C. J. Melief, Therapeutic vaccination against human papilloma virus induced malignancies. *Curr. Opin. Immunol.* 23, 252-257 (2011).
- 8 G. G. Kenter, M. J. Welters, A. R. Valentijn, M. J. Lowik, D. M. Berends-van der Meer, A. P. Vloon, F. Essahsah, L. M. Fathers, R. Offringa, J. W. Drijfhout, A. R. Wafelman, J. Oostendorp, G. J. Fleuren, S. H. van der Burg, C. J. Melief, Vaccination against HPV-16 oncoproteins for vulvar intraepithelial neoplasia. *N. Engl. J. Med.* 361, 1838-1847 (2009).
- 9 M. I. van Poelgeest, M. J. Welters, R. Vermeij, L. F. Stynenbosch, N. M. Loof, T. M. Berends-van der Meer, M. J. Lowik, I. L. Hamming, E. M. van Esch, B. W. Hellebrekers, M. van Beurden, H. W. Schreuder, M. J. Kagie, J. B. Trimbos, L. M. Fathers, T. Daemen, H. Hollema, A. R. Valentijn, J. Oostendorp, J. N. Oude Elberink, G. J. Fleuren, G. G. Kenter, T. Stijnen, H. Nijman, C. J. Melief, S. H. van der Burg, Vaccination against oncoproteins of HPV16 for non-invasive vulvar/vaginal lesions: lesion clearance is related to the strength of the T-cell response. *Clin. Cancer Res.* 22:2342-50 (2016).
- 10 M. J. Welters, G. G. Kenter, P. J. de Vos van Steenwijk, M. J. Lowik, D. M. Berends-van der Meer, F. Essahsah, L. F. Stynenbosch, A. P. Vloon, T. H. Ramwadhoebe, S. J. Piersma, J. M. van der Hulst, A. R. Valentijn, L. M. Fathers, J. W. Drijfhout, K. L. Franken, J. Oostendorp, G. J. Fleuren, C. J. Melief, S. H. van der Burg, Success or failure of vaccination for HPV16-positive vulvar lesions correlates with kinetics and phenotype of induced T-cell responses. *Proc. Natl. Acad. Sci. U.S.A.* 107, 11895-11899 (2010).
- 11 M. I. van Poelgeest, M. J. Welters, E. M. van Esch, L. F. Stynenbosch, G. Kerpershoek, E. L. van Persijn van Meerten, M. van den Hende, M. J. Lowik, D. M. Berends-van der Meer, L. M. Fathers, A. R. Valentijn, J. Oostendorp, G. J. Fleuren, C. J. Melief, G. G. Kenter, S. H. van der Burg, HPV16 synthetic long peptide (HPV16-SLP) vaccination therapy of patients with advanced or recurrent HPV16-induced gynecological carcinoma, a phase II trial. *J. Transl. Med.* 11, 88 (2013).
- 12 D. Hanahan, R. A. Weinberg, The hallmarks of cancer. *Cell* 100, 57-70 (2000).
- 13 L. Bracci, G. Schiavoni, A. Sistigu, F. Belardelli, Immune-based mechanisms of cytotoxic chemotherapy: implications for the design of novel and rationale-based combined treatments against cancer. *Cell Death Differ.* 21, 15-25 (2014).
- 14 T. C. van der Sluis, S. van Duikeran, S. Huppel-schoten, E. S. Jordanova, E. Beyranvand Nejad, A. Sloods, L. Boon, V. T. Smit, M. J. Welters, F. Oostendorp, B. van de Water, R. Arens, S. H. van der Burg, C. J. Melief, Vaccine-induced tumor necrosis factor-producing T cells synergize with Cisplatin to promote tumor cell death. *Clin. Cancer Res.* 21, 781-794 (2015).
- 15 Y. Diaz, Y. Tundidor, A. Lopez, K. Leon, Concomitant combination of active immunotherapy and carboplatin- or paclitaxel-based chemotherapy improves anti-tumor response. *Cancer Immunol. Immunother.* 62, 455-469 (2013).
- 16 A. K. Nowak, B. W. Robinson, R. A. Lake, Synergy between chemotherapy and immunotherapy in the treatment of established murine solid tumors. *Cancer Res.* 63, 4490-4496 (2003).
- 17 K. Y. Lin, F. G. Guarneri, K. F. Staveley-O'Carroll, H. I. Levitsky, J. T. August, D. M. Pardoll, T. C. Wu, Treatment of established tumors with a novel vaccine that enhances major histocompatibility class II presentation of tumor antigen. *Cancer Res.* 56, 21-26 (1996).
- 18 A. de Jong, M. I. van Poelgeest, J. M. van der Hulst, J. W. Drijfhout, G. J. Fleuren, C. J. Melief, G. Kenter, R. Offringa, S. H. van der Burg, Human papillomavirus type 16-positive cervical cancer is associated with impaired CD4+ T-cell immunity against early antigens E2 and E6. *Cancer Res.* 64, 5449-5455 (2004).
- 19 E. M. Dijkgraaf, S. J. Santeogoets, A. K. Reyners, R. Goedemans, H. W. Nijman, M. I. van Poelgeest, A. R. van Erkel, V. T. Smit, T. A. Daemen, J. J. van der

- S. H. van der Burg, A phase 1/2 study combining gemcitabine, Pegintron and p53 SLP vaccine in patients with platinum-resistant ovarian cancer. *Oncotarget* 6: 32228-43 (2015).
- 21 M. L. Talebian Yazdi, N. M. Loof, K. L. Franken, C. Taube, J. Oostendorp, P. S. Hiemstra, M. J. Welters, S. H. van der Burg, Local and systemic XAGE-1b specific immunity in patients with lung adenocarcinoma. *Cancer Immunol. Immunother.* 64, 1109-1121 (2015).
 - 22 S. Walter, T. Weinschenk, A. Stenzl, R. Zdrojowy, A. Pluzanska, C. Szczylik, M. Staehler, W. Brugger, P.Y. Dietrich, R. Mendrzyk, N. Hilf, O. Schoor, J. Fritsche, A. Mahr, D. Maurer, V. Vass, C. Trautwein, P. Lewandrowski, C. Flohr, H. Pohla, J.J. Stanczak, V. Bronte, S. Mandruzzato, T. Biedermann, G. Pawelec, E. Derhovanessian, H. Yamagishi, T. Miki, F. Hongo, N. Takaha, K. Hirakawa, H. Tanaka, S. Stevanovic, J. Frisch, A. Mayer-Mokler, A. Kirner, H. G. Rammensee, C. Reinhardt, H. Singh-Jasuja, H. Multiple-peptide immune response to cancer vaccine IMA901 after single-dose cyclophosphamide associates with longer patient survival. *Nat. Med.* 18, 1254-1261 (2012).
 - 23 J. M. Nabholz, K. Gelmon, M. Bontenbal, M. Spielmann, G. Catimel, P. Conte, U. Klaassen, M. Namer, J. Bonnetterre, P. Fumoleau, B. Winograd, Multicenter, randomized comparative study of two doses of paclitaxel in patients with metastatic breast cancer. *J. Clin. Oncol.* 14, 1858-1867 (1996).
 - 24 C. H. Yarbrow, Carboplatin: a clinical review. *Semin. Oncol. Nurs.* 5, 63-69 (1989).
 - 25 W. C. Rose, J. E. Schurig, Preclinical antitumor and toxicologic profile of carboplatin. *Cancer Treat Rev.* 12 (Suppl A), 1-19 (1985).
 - 26 M. Treskes, E. Boven, A. A. van de Loosdrecht, J. F. Wijffels, J. Cloos, G. J. Peters, H. M. Pinedo, W. J. van der Vijgh, Effects of the modulating agent WR2721 on myelotoxicity and antitumour activity in carboplatin-treated mice. *Eur. J. Cancer.* 30A, 183-187 (1994).
 - 27 H. Minami, Y. Sasaki, N. Saijo, T. Ohtsu, H. Fujii, T. Igarashi, K. Itoh, Indirect-response model for the time course of leukopenia with anticancer drugs. *Clin. Pharmacol. Ther.* 64, 511-521 (1998).
 - 28 W. Krzyzanski, W. J. Jusko, Multiple-pool cell lifespan model of hematologic effects of anticancer agents. *J. Pharmacokinetic. Pharmacodyn.* 29, 311-337 (2002).
 - 29 S. Coleman, A. Clayton, M. D. Mason, B. Jasani, M. Adams, Z. Tabi, Recovery of CD8+ T-cell function during systemic chemotherapy in advanced ovarian cancer. *Cancer Res.* 65, 7000-7006 (2005).
 - 30 X. Wu, Q. M. Feng, Y. Wang, J. Shi, H. L. Ge, W. Di, The immunologic aspects in advanced ovarian cancer patients treated with paclitaxel and carboplatin chemotherapy. *Cancer Immunol. Immunother.* 59, 279-291 (2010).
 - 31 S. Mabuchi, Y. Matsumoto, F. Isohashi, Y. Yoshioka, H. Ohashi, E. Morii, T. Hamasaki, K. Aozasa, D. G. Mutch, T. Kimura, Pretreatment leukocytosis is an indicator of poor prognosis in patients with cervical cancer. *Gynecol. Oncol.* 122, 25-32 (2011).
 - 32 S. C. Stone, R. A. Rossetti, A. Bolpetti, E. Boccardo, P. S. Souza, A. P. Lepique, HPV16-associated tumors control myeloid cell homeostasis in lymphoid organs, generating a suppressor environment for T cells. *J. Leukoc. Biol.* 96, 619-631 (2014).
 - 33 M. Reck, I. Bondarenko, A. Luf, P. Serwatowski, F. Barlesi, R. Chacko, M. Sebastian, H. Lu, J. M. Cuillerot, T. J. Lynch, Ipilimumab in combination with paclitaxel and carboplatin as first-line therapy in extensive-disease-small-cell lung cancer: results from a randomized, double-blind, multicenter phase 2 trial. *Ann. Oncol.* 24, 75-83 (2013).
 - 34 P. J. de Vos van Steenwijk, T. H. Ramwadhoebe, R. Goedemans, E. M. Doorduijn, J. J. van Ham, A. Gorter, T. van Hall, M. L. Kuijjer, M. I. van Poelgeest, S. H. van der Burg, E. S. Jordanova, Tumor-infiltrating CD14-positive myeloid cells and CD8-positive T-cells prolong survival in patients with cervical carcinoma. *Int. J. Cancer.* 133, 2884-2894 (2013).
 - 35 M. C. A. D. Wouters, E.M; Kuijjer, M.L; Jordanova, E.S; Hollema, H.; Welters, M.J.P.; van der Hoeven, J.J.M.; Daemen, T.; Kroep, J.R; Nijman, H.W.; van der Burg, S.H.; Interleukin-6 receptor and its ligand interleukin-6 are opposite markers for survival and infiltration with mature myeloid cells in ovarian cancer. *Oncimmunology* 3, (2014)
 - 36 G. I. W. G. European Medicines Agency, Reflection paper for laboratories that perform the analysis or evaluation of clinical trial samples, 19 (2012).

Figure 1 CarboTaxol improves the clinical outcome of therapeutic peptide vaccination. (A) c57BL/6 mice were injected with 1×10^5 TC-1 tumor cells and treated systemically with carboplatin (C) and paclitaxel (P) with or without injection of the HPV16 E7₄₃₋₇₇ peptide in Montanide vaccine (V) in the flank opposite of the tumor as shown in the schematic diagram. (B) Kaplan-Meier survival plots show the combined data from several experiments (number of mice is indicated). Peptide vs peptide-CarboTaxol treated group ($p = 0.004$). (C) Tumor growth data from two pooled individual experiments with eight mice per group. Quantification of the percentage of (D) CD4⁺ T-cells, (E) CD8⁺ T-cells, and (F) the vaccine-specific CD8⁺ T-cells as determined by H2-Db E7₄₉₋₅₇ (RAHYNIVTF) tetramer (TM) staining. Column 3 vs 1 ($p = 0.03$), 2 and 4 ($p = 0.005$). Column 5 vs 2 and 4 ($p = 0.03$). $N = 8$ mice in the tumor-bearing groups, $N = 4$ in the naïve group, data are representative of two individual experiments and expressed as mean plus standard error of the mean (SEM). Data were analyzed by one-way ANOVA followed by Tukey's post-hoc analysis.

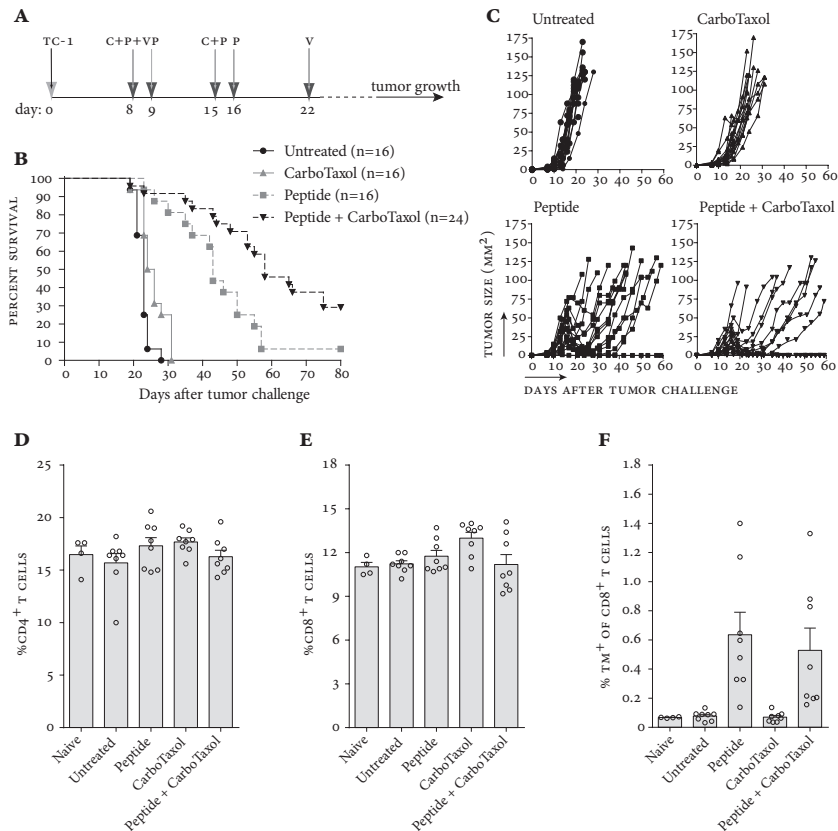
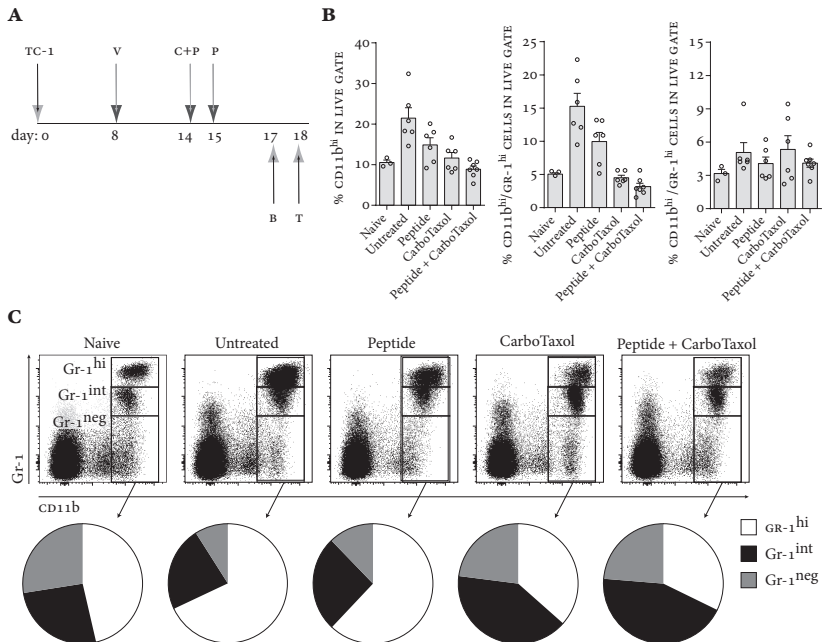


Figure 2 Chemotherapy normalizes systemic tumor-induced myeloid subsets, but intra-tumoral τ -cells are not affected. (A) C57BL/6 mice were injected with TC-1 tumor cells (TC-1) and treated with HPV16 E7₄₃₋₇₇ peptide in Montanide vaccine (V) in the flank opposite of the tumor and with carboplatin (C) and paclitaxel (P) as indicated in the schematic diagram. B and T indicate the time points for blood and tumor analysis, respectively. (B) Flow cytometry analysis of the total percentage of myeloid cells [left; column 2 vs 1 ($p = 0.007$), 4 ($p = 0.003$) and 5 ($p < 0.0001$)], the CD11b^{hi}Gr-1^{hi} cells [middle; column 2 vs 1 ($p = 0.0004$), 3, ($p = 0.03$), 4 and 5 ($p < 0.0001$); column 3 vs 4 ($p = 0.02$) and 5 ($p = 0.002$)], and the CD11b^{hi}Gr-1^{int} (right) cells in the blood. (C) Representative flow cytometry plots for each treatment, gated on live (γ AAD⁻) cells (top). Distribution of Gr-1^{hi}, Gr-1^{int}, and Gr-1^{neg} expressing cells within the total CD11b^{hi} population is indicated in the pie charts (bottom). Tumor samples were collected and analyzed to determine the percentage of



(D) CD45⁺ cells within the live gate [Column 1 vs 2 and 4 ($p < 0.0001$) and 3 ($p = 0.02$); column 3 vs 2 and 4 ($p < 0.0001$)], (E) CD8⁺ T-cells in the leukocyte gate [Column 1 vs 2 and 4 ($p < 0.0001$); column 3 vs 2 and 4 ($p < 0.0001$)], (F) vaccine-specific T-cells determined by H2-D^b E7₄₉₋₅₇ (RAHYNIVTF) tetramer staining [Column 1 vs 2 and 4 ($p < 0.0001$); column 3 vs 2 and 4 ($p < 0.0001$)]. (G) Single cell suspensions of tumors were co-incubated with HPV16 E7₄₃₋₇₇ peptide-pulsed D1 cells and stained for intracellular TNF α and IFN- γ . Representative flow cytometry plots (left) and quantification (right) show the frequency of cytokine-producing CD8⁺ T-cells [IFN- γ graph: column 1 vs 2 ($p = 0.009$) and 4 ($p = 0.0001$); column 3 vs 2 ($p = 0.004$) and 4 ($p < 0.0001$). TNF α graph: column 1 vs 2 ($p = 0.006$) and 4 ($p = 0.009$); column 3 vs 2 ($p = 0.009$) and 4 ($p = 0.001$)]. N = 5-7 mice per group, data shown are representative of two individual experiments. Data are expressed as mean plus SEM and analyzed by one-way ANOVA followed by Tukey's post-hoc analysis.

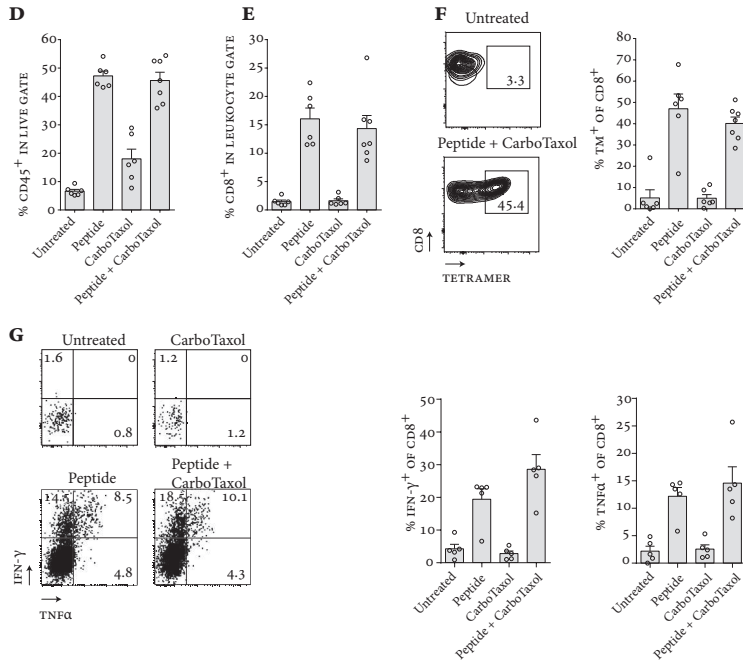


Figure 3 Gr-1^{hi} cells are depleted from the tumor by CarboTaxol treatment. Mice were treated as in figure 2. Tumor samples were isolated and analyzed by flow cytometry. **(A)** Leukocytes from resected untreated tumors were analyzed for the expression of Gr-1 and CD11b. The histograms show the expression of class II, CD80, CD86, F4/80, Ly6G, and CD11c on the Gr-1^{hi} (gray lines) and Gr-1^{int} (black lines) subsets. **(B)** Four days after chemotherapy or ten days after peptide vaccination, leukocytes from resected tumors were analyzed for the expression of Gr-1 and CD11b (top). Distribution of Gr-1^{hi}, Gr-1^{int}, and Gr-1^{neg} expressing cells within the total CD11b^{hi} population is shown in the pie charts (bottom). **(C)** Percentages (mean plus SEM) of Gr-1^{hi} [Column 1 vs 2 ($p = 0.006$), 3 ($p = 0.0004$) and 4 ($p = 0.0008$)] and Gr-1^{int} [Column 4 vs 1 ($p = 0.0006$) and 2 ($p = 0.02$)] subsets were analyzed for untreated and treated tumors. $N = 5-7$ mice per group, data shown are representative of two individual experiments. Data were analyzed by one-way ANOVA followed by Tukey's post-hoc analysis.

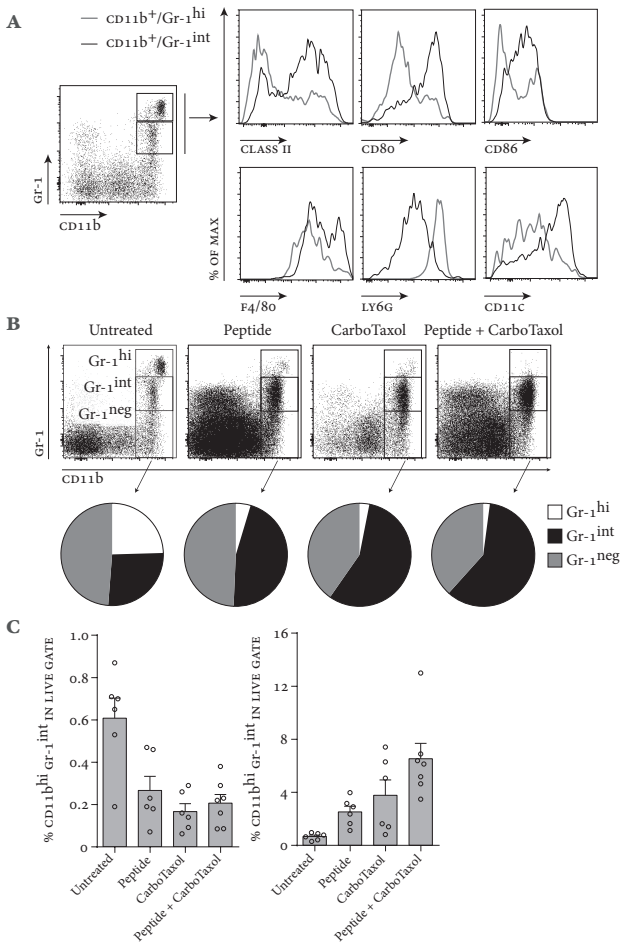


Figure 4 CarboTaxol induces changes in cellular immunity in advanced stage cervical cancer patients. (A) Blood draws (B) and CarboTaxol cycles (C) for the 6 patients in cohort 1 are indicated in days (D) and weeks (W) in the schematic outline. (B) Representative flow cytometry plots show the myeloid cell gate and lymphocyte gate in the blood of a patient at baseline and after 1 to 2 CarboTaxol cycles in comparison to the blood of a healthy donor. The percentages of myeloid cells and lymphoid cells within the total number of cells are indicated. To determine the relative percentage of each population, the sum of the events in the lymphoid and myeloid cell gates in the forward and side scatter plots was set to 100 and then the frequency of (C) myeloid cells [column 1 vs 4 ($p = 0.0002$), 5 ($p = 0.02$), and 6 ($p = 0.005$)] and of (D) lymphocytes [column 1 vs 4 ($p = 0.0002$), 5 ($p = 0.02$), and 6 ($p = 0.005$)] was determined. (E) Proliferation of T-cells upon recognition of recall antigens (memory response mix, MRM) shown as stimulation index. Column 1 vs 3 and 6 ($p = 0.02$), 4 ($p = 0.001$), and 5 ($p = 0.005$). (F) The ability of antigen presenting cells to stimulate T-cells in a mixed lymphocyte reaction shown for the 4 tested patients. Column 1 vs 2 ($p = 0.005$) and 4 ($p = 0.049$). Data (shown as median plus interquartile range) were analyzed by repeated measures model.

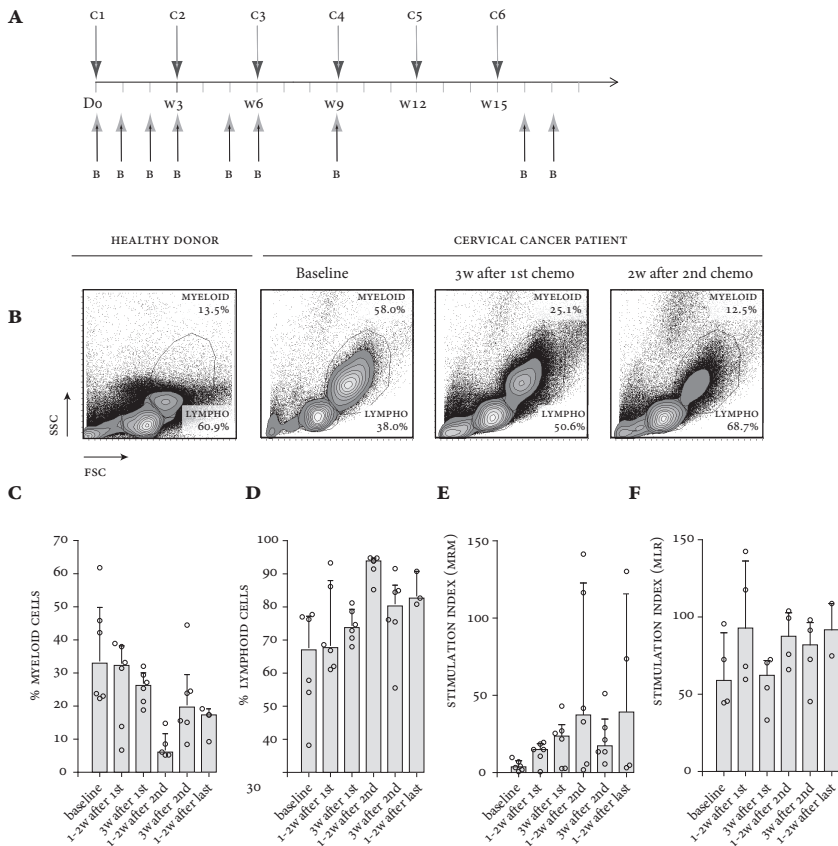


Figure 5 The frequencies of circulating immune cells normalize upon CarboTaxol treatment. Blood samples of the 12 patients in cohort 2 were analyzed for leukocyte differentiation, showing a shift from baseline for the counts of **(A)** lymphocytes and **(B)** leukocytes $\times 10^9/L$. Column 1 vs 3 ($p = 0.007$) and 4 to 6 ($p < 0.0001$), 5 ($p = 0.04$) and 6 ($p = 0.003$). The frequency of **(C)** myeloid cells [Column 1 vs 2 ($p < 0.0001$), 3 ($p = 0.002$), 4 ($p = 0.003$), 5 ($p = 0.006$), 6 ($p = 0.008$) and 7 ($p = 0.009$); column 2 vs 3 ($p = 0.04$), 4 ($p = 0.02$), 5 ($p = 0.007$), 6 and 7 ($p = 0.004$)] and **(D)** lymphocytes [Column 1 vs 2 ($p < 0.0001$), 3 ($p = 0.0004$), 4 ($p = 0.0009$), 5 ($p = 0.002$), 6 ($p = 0.005$) and 7 ($p = 0.006$); column 2 vs 3 ($p = 0.02$), 4 ($p = 0.002$), 5 ($p = 0.0009$), 6 and 7 ($p = 0.0002$)] were determined in the forward and side scatter plots of these blood samples after acquisition by flow cytometry. Blood samples from healthy donors (HD, $n = 19$) were included for comparison. Data (shown as median plus interquartile range) were analyzed by repeated measures model. The fold change in stimulation index (SI), which is SI in a sample during/after chemotherapy divided by that of the baseline sample, of the blood samples stimulated with **(E)** recall antigens (MRM) or **(F)** Influenza Matrix 1 peptides (FLU) is shown vs the shift in percentage of myeloid or lymphoid cells from baseline. Repeated measures regression analysis was conducted to determine whether there is a slope significantly different from 0, represented with the p-value.

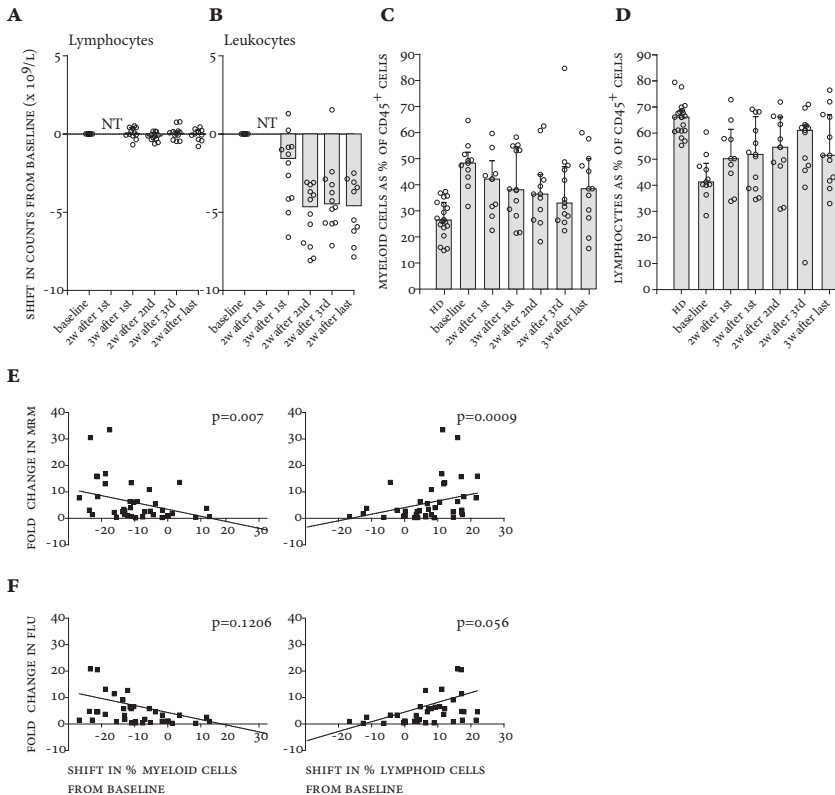


Figure 6 CarboTaxol treatment induces a decline in all subsets of circulating myeloid cells.

PBMC from the 12 patients in cohort 2 were subjected to multi-parameter flow cytometry analysis. (A) Representative dot plots of the five subpopulations within the $CD45^+CD3^-CD19^-CD1a^-HLA-DR^+$ population defined by expression of $CD11b$ and $CD14$ in the baseline blood sample and 2 weeks after the second cycle of chemotherapy. (B) The frequency of $(CD45^+CD3^-CD19^-CD1a^-HLA-DR^+)$ $CD11b^+CD14^+$ (population 1) as a percentage of the $CD45^+$ cells in healthy donors (HD, $N = 19$) and in the patients over time. The time points of blood sampling (X-axis) were 2 weeks after the first (1^{st}), second (2^{nd}), and third (3^{rd}) cycle of chemotherapy and 3 weeks after the sixth (6^{th}) or last chemotherapy cycle. Column 1 vs 2 ($p < 0.0001$), 3 ($p = 0.01$), 4 ($p = 0.02$), 5 ($p = 0.009$) and 6 ($p = 0.04$). Column 2 vs 3 ($p = 0.04$), 4 ($p = 0.01$), 5 ($p = 0.02$) and 6 ($p = 0.005$). (C) The fold change in stimulation index (SI) of the blood samples stimulated with recall antigens (MRM) or Influenza Matrix 1 peptides (FLU) is shown vs the absolute shift in percentage of population 1 cells from baseline. Repeated measures regression analysis was conducted to determine whether there is a slope significantly different from 0, represented with the p-value. The frequencies of (D) $CD163^-CD206^-CD16^-CD11c^+$ [M1-like cells; column 1 vs 2 ($p = 0.001$) and 3 ($p = 0.01$); column 2 vs 5 ($p = 0.01$)] and (E) $CD163^+CD206^-CD16^-CD11c^+$ [M2c-like cells; column 1 vs 2 ($p = 0.004$) and 5 ($p = 0.01$)] within population 1 are shown for the healthy donors and patients over time. (F) The frequency of myeloid-derived suppressor cells (MDSCs; $CD45^+CD3^-CD19^-CD1a^-HLA-DR^+/low$) is depicted. Column 1 vs 3 ($p = 0.03$). Column 2 vs 4 ($p = 0.04$). Data (shown as median plus interquartile range) were analyzed by repeated measures model.

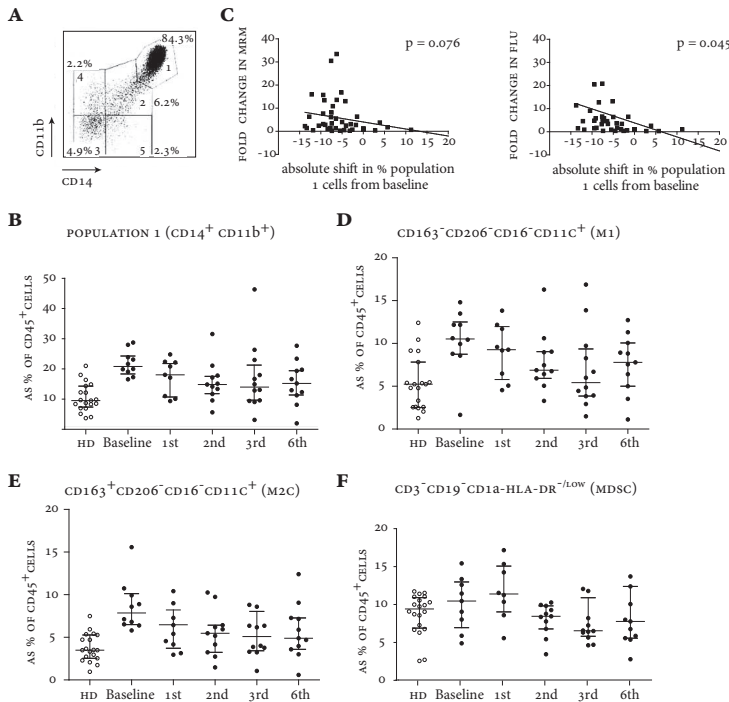
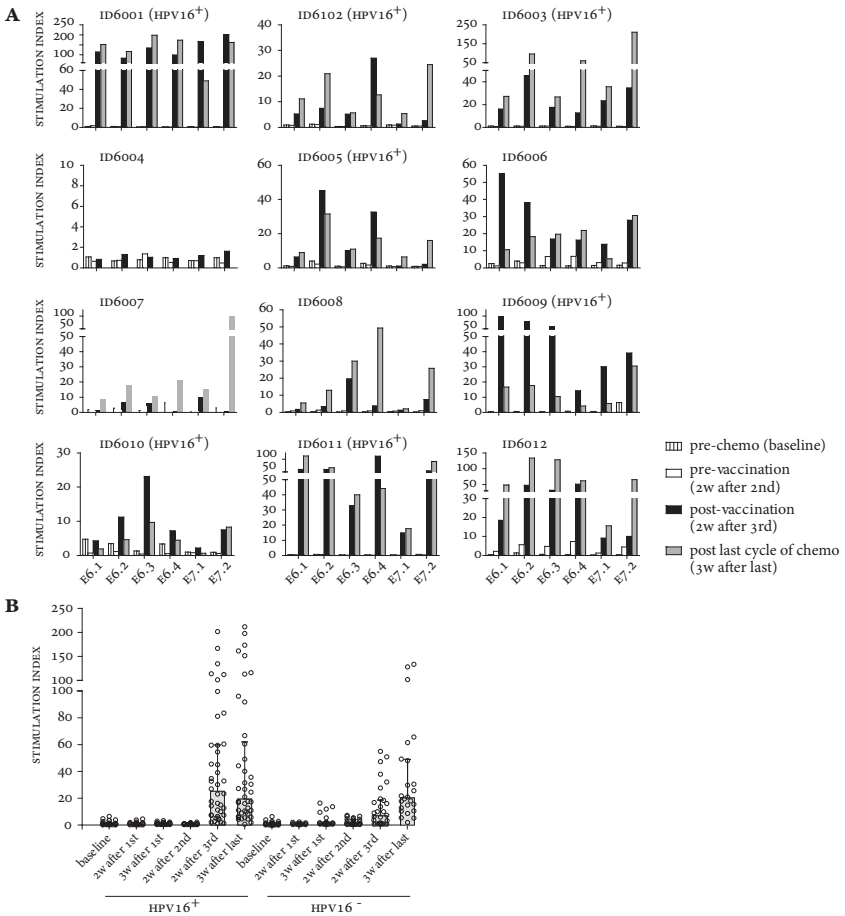


Figure 7 HPV16 SLP vaccination during CarboTaxol treatment results in a strong immune response in patients. The patients in cohort 2 received a single vaccination with HPV16-SLP subcutaneously at 2 weeks after the second cycle of chemotherapy. **(A)** The proliferative responses of T-cells in the lymphocyte stimulation test (LST) are shown as a stimulation index and depicted vs the indicated peptide pools used for stimulation of the cells in the blood sample at baseline (hatched bar), 2 weeks after the second cycle of chemotherapy and before vaccination (white bar), 3 weeks after this single vaccination (black bar), and 3 weeks after the sixth or last cycle of chemotherapy (gray bar). **(B)** The patients are grouped by HPV16 status (HPV16⁺, N = 7; HPV16⁻, N = 5), and the proliferative response (stimulation index) is plotted vs the indicated blood samples. Each dot represents one response against HPV16 E6 and E7. In total 6 peptide pools were tested per blood sample. Data were analyzed by linear mixed model analysis and showed no statistically significant difference.



SUPPLEMENTAL INFORMATION

ANALYSIS OF MURINE TUMOR INFILTRATING IMMUNE POPULATIONS

TC-1 tumor-bearing mice were injected with synthetic long HPV16 E7₄₃₋₇₇ peptide in the contralateral flank. Chemotherapy was provided intraperitoneally (i.p.) on day 14 (carboplatin) and day 14 and 15 (paclitaxel). On day 17, blood was taken and analyzed by flow cytometry. Tumor-infiltrating immune populations were analyzed as previously described.¹³ Briefly, single cell suspensions of tumors from transcardially perfused mice were incubated with 7-Aminoactinomycin D (Life Technologies) to exclude dead cells, with H-2D^b tetramers containing HPV16 E7₄₉₋₅₇ peptide (RAHYNIVTF) labeled with APC, and with the indicated antibodies from Biolegend: Gr-1-PE Cy7 (clone RB6-8C5), Ly6G-Alexa Fluor 700 (AF700; clone 1A8), CD4-BV605 (clone L3T4); eBioscience: CD11b-Pacific Blue (PC; clone M1/70), F4/80-PE (clone BM8), CD80-FITC (clone 16-10A1), CD86-PE (clone GL1, BD), CD3-PE Cy7 (clone 145-2C11), CD8a-AF700 (clone 53-6.7), CD45.2 eFluor 780 (clone 104) and CD19-APC (clone 1D3); or BD: MHC-class II-Horizon v500 (HV500; clone M5/114.15.2, BD), CD11c Brilliant Violet 605 (BV605; clone HL3, BD).

To determine the capacity of cells to produce pro-inflammatory cytokines, single cell suspensions of tumor infiltrating cells were incubated for 5 hours with 40,000 D1 dendritic cells pre-loaded with HPV16 E7₄₃₋₇₇ peptide (10 µg/ml) in the presence of Brefeldin A (2 µg/ml, Sigma). After cell surface staining with fluorescently labelled antibodies to mouse CD45, CD8, and CD3, overnight fixation with 0.5% paraformaldehyde solution (Pharmacy LUMC), and permeabilization with Perm/Wash buffer (BD), the cells were stained at 4°C with antibodies against IFN-γ (APC, clone XMG1.2, eBioscience) and TNFα (FITC, clone MP6-XT22, eBioscience).

IMMUNOMONITORING OF BLOOD SAMPLES FROM CERVICAL CANCER PATIENTS

THE SAMPLES Venous blood samples (45 mL in heparinized tubes and 8.5 mL in clot activator tube) were taken for immunomonitoring before chemotherapy (baseline), 1 or 2 weeks after the first cycle of chemotherapy (1-2 wk after 1st), before (3 wk after 1st) and 1 to 2 weeks after the second cycle (1-2wk after 2nd), 2-3 weeks after the 3rd cycle (2-3wk after 3rd), and 1-2 or 3 weeks after the last cycle indicated in table S1 (maximum 6th cycle; 1-2 or 3 wk after last) of chemotherapy (figure 4A). In addition, blood samples (50 mL) were drawn from 19 healthy blood donor volunteers (≥ 18 years old females) after they had signed an informed consent. The blood (transported at room temperature) was processed within 3 hours and peripheral blood mononuclear cells (PBMCs) were isolated by Ficoll gradient centrifugation, washed, partly used in the lymphocyte

stimulation test (LST), and the remaining cells were cryopreserved in 90% fetal calf serum (PAA Laboratories) and 10% DMSO at a concentration of 7-12 million cells per vial in a total volume of 1 mL) using a Mr. Frosty's freezing container (Nalgene). Upon cryopreservation the vials were stored in the vapor phase of the liquid nitrogen until further use.

THE ASSAYS

PROLIFERATION ASSAYS The HPV16-specific proliferative response was determined using freshly isolated PBMCs that were subjected to the LST as described previously.⁸⁻¹¹ In brief, eight replicate wells with 1.5×10^5 cells per well were stimulated for 6 days with HPV16 E6 or E7 peptide pools (10 $\mu\text{g}/\text{mL}$ per peptide), after which 50 μL supernatant per well was harvested and stored at -20°C for cytokine analysis. The cells were pulsed with [^3H]-Thymidine (Perkin Elmer) for 16 hours and harvested, and uptake was determined by Wallac Microbetatriliux (Perkin Elmer). As a positive control, the previously described memory response mix (MRM) and influenza matrix 1 protein-derived overlapping peptides (FLU) were used.¹³ The negative control consisted of cells in medium only. A positive response was defined as a stimulation index (SI) of at least 3 under the condition that 6 out of the 8 wells displayed values above the cut-off, which was defined as the mean value of the cells in medium only plus 3 standard deviations (SD).

The capacity to respond to phytohemagglutinin (PHA) was studied using cryopreserved PBMCs. Cells were thawed and tested in a 3-day proliferation assay as described previously³³, with the minor alteration that now 50,000 cells per well (in quadruplicate) were incubated in medium (IMDM, Lonza) or stimulated with 0.5 $\mu\text{g}/\text{mL}$ PHA (Murex Biotech HA16). A positive response was defined as an SI of at least 3.

The antigen-presenting capacity of the PBMC samples from patients was determined in a mixed lymphocyte reaction (MLR).³⁴ Patients' PBMCs were thawed in Iscove's Modified Dulbecco's Medium (IMDM) plus 10% fetal bovine serum and 30 mg/ml DNase, resuspended in IMDM plus 10% human AB serum, irradiated (3000 rad) to prevent proliferation, washed, and resuspended in IMDM plus 10% human AB serum and then plated at 1×10^5 cells per well (in quadruplicate). Third party PBMCs were added (1×10^5 million cells/well), making a total volume of 200 $\mu\text{L}/\text{well}$. Irradiated PBMCs alone as well as third party PBMCs alone were used as negative controls. At day 6, 100 μL supernatant per well was harvested for cytokine analysis, and the cells were subjected to [^3H]-Thymidine (50 $\mu\text{L}/\text{well}$ of 10 $\mu\text{Ci}/\text{mL}$) for an additional 16 hours. A positive response was defined as an SI of at least 3.

MYELOID CELL DEPLETION AND STIMULATION OF PBMCs IN VITRO The CD14⁺ myeloid cells in PBMCs of 2 cervical cancer patients were depleted by magnetic cell sorting (Miltenyi) as described earlier.²⁸ Depleted and non-depleted PBMC were stimulated for 11 days with autologous monocytes pulsed with either a mix of overlapping FLU peptides and MRM,⁹⁻¹¹ a mix of HPV16 E6/E7 SLP (32-35 amino acid long overlapping peptides³³), or a mix of p53 SLP (30-mer overlapping peptides) and then tested in a proliferation test (triplicate wells) as described above, with non-pulsed autologous monocytes serving as a negative control.²⁸

CYTOKINE ANALYSIS The supernatants of the LST, PHA, and MLR proliferation assays were used for cytokine analysis with a flow cytometer-based cytokine bead array (CBA, human Th1/Th2 kit, BD) according to the manufacturer's instructions as reported earlier.⁹⁻¹¹ The cytokines measured by this kit were IFN- γ , TNF α , IL-10, IL-5, IL-4, and IL-2. A positive response was defined as being above the detection limit, which is 20 pg/mL for each of the cytokines. A three-fold increase above the baseline sample (pre-treatment) was defined as a treatment-related change.

PHENOTYPING OF PMBCS The PBMC samples isolated at different time points during treatment were phenotyped with 4 sets of 6-11 cell surface markers to identify macrophages, myeloid derived suppressor cells (MDSCs), and the expression of co-inhibitory molecules and regulatory t-cells by flow cytometry.³⁴

The macrophage set consisted of CD3-PB (Clone UCHT1; Dako), CD1a-FITC (Clone HI149; BD), CD11b-PE (Clone D12; BD), CD11c-AF700 (Clone b-Ly6; BD), CD14-PE CY7 (Clone M5E2; BD), CD16-PE CF594 (Clone 3G8; BD), CD19-BV605 (BV605, Clone SJ25C1; BD), CD45-PerCP Cy5.5 (Clone 2D1; BD), CD163-APC (Clone 215927; R&D), CD206-APC CY7 (Clone 15-2; Biolegend), and HLA-DR HV500 (Clone L243; BD).

The MDSC set contained the same CD3-PB, CD19-BV605, CD45-PerCP Cy5.5, and HLA-DR HV500 antibodies and additionally CD11b-FITC (Clone CBRm1/5; Biolegend), CD14-AF700 (Clone M5E2; BD), CD15-PE CF594 (Clone w6D3; BD), CD33-PE CY7 (Clone P67.6; BD), CD34-APC (Clone 581; BD), and CD124-PE (Clone HIL4R-M57; BD).

The inhibitory set consisted of the same antibody as above for CD3, and additionally CD4-PE CF594 (Clone RPA-T4; BD), CD8-APC CY7 (Clone SK1; BD), CD152-PE Cy5 (anti-CTLA-4; Clone BN13, BD), CD279-BV605 (anti-PD-1; Clone EH12.2H7; Biolegend), and TIM3-PE (Clone F38-2E2; Biolegend).

The regulatory T-cell set consisted of CD3-HV500 (Clone UCHT1; BD), CD4-AF700 (Clone RPA-T4; BD), CD8-PerCP Cy5.5 (clone SK1; BD), CD25-PE Cy7 (clone 2A3; BD), CD127-BV650 (clone HIL-7R-m21; BD), Foxp3-PE CF594 (clone 259D/C7; BD), Ki67-FITC (clone 20Raj1; eBioscience), CD45-RA-APC H7 (clone HI100; BD), and live/dead marker (Yellow Amino Reactive Dye (ARD), Life Technologies).

The sets of markers for MDSCs and regulatory t-cells were selected according to the consensus within the CIMT immunoguiding program (CIP).

The cryopreserved PBMCs were thawed and stained. Briefly, for the staining of surface markers the cells were washed in phosphate buffered saline (PBS) supplemented with 0.5% bovine serum albumin (BSA, Sigma), incubated for 10 min at room temperature (RT) in PBS/0.5% BSA/10%FCS (in the dark) to prevent non-specific antibody binding, centrifuged, resuspended in the antibody mixtures described above and incubated for 30 min on ice (in the dark). Then, the cells were washed twice with PBS/0.5% BSA and finally resuspended in 1% paraformaldehyde (Pharmacy LUMC). For the regulatory t-cell staining, the cells were first subjected to Yellow ARD (20 minutes at RT in 100 μ L/well of 1:800 diluted Yellow ARD), blocked for non-specific staining, and subsequently stained for surface markers as described above, followed by washing in transcription factor fixation and permeabilization buffer (BD) and staining with the intranuclear antibodies for Foxp3 and Ki67 diluted in permeabilization and washing buffer (BD) for 40-50 minutes at 40 C. The cells were then resuspended in 1% paraformaldehyde and analyzed within 24 hours while keeping at 4° C.

INTRACELLULAR CYTOKINE STAINING (ICS)

For the simultaneous detection of surface markers (CD3, CD4, CD8), activation markers (CD154, CD137), and intracellular cytokines (IFN- γ and IL-2), the PBMCs were subjected to the direct ex-vivo multiparameter flow cytometry assay as described previously.⁹ Cells in medium only and cells stimulated overnight with Staphylococcal Enterotoxin B (2 μ g/mL; Sigma) were taken along as negative and positive control, respectively. A positive response was defined as twice the level of the negative control and at least 10 events in the gate. A vaccine-induced response required at least a 3-fold increase in reactivity compared to the baseline sample.

FLOW CYTOMETRY The acquisition on the Fortessa or LSRII (BD) flow cytometers was performed < 24 hours after the staining was finished. Analysis was performed by using FlowJo (Tree Star; Version 10) or DIVA software (Version 6.2).

LABORATORY ENVIRONMENT Immunomonitoring of patients' PBMCs was performed in the laboratory of the department of Clinical Oncology (LUMC) that operates under research conditions but uses standard operation procedures for all tests, with pre-established definitions of positive responses and trained personnel. This laboratory has been externally and internally audited according to the reflection paper for laboratories that perform immunomonitoring³⁵ and participated in all proficiency panels of the CIMT Immunoguiding Program (CIP; of which SHVDB and MJPW are steering committee members; <http://www.cimt.eu/workgroups/cip/>) as well as many of the proficiency panels (including ICS gating and ELISPOT plate reading panels) of the USA-based Cancer Immunotherapy Consortium (CIC of the Cancer Research Institute) to validate its standard operating procedures (SOPs).

STATISTICAL ANALYSIS

Survival of differentially treated tumor-bearing mice was compared by the Kaplan-Meier method and the log-rank (Mantel-Cox) test. Statistical analysis of immune parameters in mice was performed with one-way ANOVA followed by Tukey's post-hoc analysis. Statistical analysis was performed in GraphPad Prism software (version 6).

The immune responses of patients were analyzed with a repeated measures model with fixed factors group, time and group by time, and repeated time within the patient group. The Kenward-Roger approximation was used to estimate denominator degrees of freedom, and model parameters were estimated using the restricted maximum likelihood method. Residual graphs were used to decide which variables would be log transformed before analysis to correct for the expected log-normal distribution of the data. The general group effect was calculated within the model as the average least square means (LSM) over all time points for the patients versus the LSM of the healthy donors. If the general group effect was significant ($p < 0.05$), the various differences (healthy donors vs patients at each time point) were calculated. In a separate analysis with patient data, only the general time effect within patients was estimated. If the time effect was significant ($p < 0.05$), the various differences between time points within the patient group were calculated within the original model. The fold change in MRM and FLU and absolute shift in myeloid, lymphoid, and population 1 cells was analyzed with a repeated measures regression analysis with a compound covariance structure and time as repeated factor within subject. Because the number of myeloid cells reached its nadir after 2 cycles of CarboTaxol and was retained throughout the treatment, the results of patient

ID6008, who received the vaccine after the third cycle, were used as if this patient was vaccinated in the same time window as the others. A p-value < 0.05 was considered statistically significant. Statistical analysis was performed using SAS for windows v9.4 (SAS Institute, Inc.). To determine whether a significant difference existed between the patients with a HPV16 positive cervical tumor and those with a HPV16 negative (other HPV type) tumor in the proliferative response to the 6 tested HPV16 peptide pools, we used a mixed linear model with unstructured correlation metric as covariance type using SPSS statistics (version 20). In this model, the possible link between the different peptide pools (although biologically unrelated) was incorporated when the peptide pool was taken as a dependent variable.

Table s1 Patient characteristics. Age at diagnosis (D) of cervical cancer. Age at first recurrence (R), metastatic disease or advanced stage of disease. Age at which the patient was included (I) in the trial, this equals the age at the start of chemotherapy CarboTaxol.

ID	Age			Primary Tumor		Advanced / Recurrent / metastatic disease		
	D	R	I	FIGO	Treatment	Disease	Interval P-R (months)	Prior treatments
1	51	52	52	IIB	CHRT	recurrent	6	none
2	60	60	60	IV	CHRT	advanced	n.a.	n.a.
3	32	38	39	IB2	SUR + RT	metastatic	73	CH+RT+HT (cisplatin)
4	45	49	50	IB1	SUR + RT	metastatic + recurrent	47	RT
5	55	56	56	IIA	SUR + RT	metastatic	18	none
6	36	36	36	IIIB	CHRT	metastatic	8	none
6001	50	50	50	IV	CH	advanced	N.A.	N.A.
6002	54	56	56	IB1	SUR + RT	metastatic	24	CT + RT (cisplatin)
6102	47	48	48	IB1	SUR + CHRT	recurrent	14	none
6003	42	45	45	IB1	SUR + CHRT	metastatic	35	none
6004	32	33	33	IIB	RT + BT + HT	recurrent	5	none
6005	35	37	37	IB1	SUR	recurrent	22	none
6006	34	35	36	IIB	CHRT + HT	recurrent	22	alternative
6007	49	55	55	IB1	SUR + CHRT	recurrent	64	none
6008	70	71	71	IIIB	RT + BT + HT	metastatic	21	none
6009	29	34	34	IA1	SUR	metastatic	56	none
6010	33	36	37	IIB	SUR + CHRT	metastatic	37	CT + RT (cisplatin)
6011	28	29	31	IB1	SUR	metastatic + recurrent	16	RT
6012	58	58	58	IV	CH	advanced	N.A.	N.A.

Vaccination						
No. of cycles CarboTaxol	Dose Carboplatin	Dose Paclitaxel	Tumor HPV type	Interval CH-vacc (days)	Interval vacc-CH (days)	No. of vacc.
3	normal	normal	16	N.A.	N.A.	0
6	reduced	reduced	16	N.A.	N.A.	0
6	normal	normal	18	N.A.	N.A.	0
6	normal	normal	16	N.A.	N.A.	0
6	normal	normal	16	N.A.	N.A.	0
5	normal	normal	16	N.A.	N.A.	0
6	normal	normal	16	17	6	1
1	normal	normal	16	N.A.	N.A.	0
6	normal	normal	16	18	3	1
6	normal	normal	16	13	8	1
3	normal	normal	-#	15	6	1
6	normal	normal	16	15	6	1
6	reduced	reduced	-	14	15	1
6	normal	normal	-	15	6	1
6	reduced	reduced	-	17*	15§	1
6	normal	normal	16	15	6	1
6	normal	normal	16	13	8	1
6	normal	normal	16	15	6	1
6	normal	normal	-	17	4	1

* For patient ID6008, vaccination took place 17 days after the 3rd cycle of chemotherapy with CarboTaxol (vaccination was postponed due to infection). # HPV16 negative, but not tested for other high-risk HPV types. FIGO: International Federation of Gynecology and Obstetrics representing stage of cancer at diagnosis; CHRT: chemoradiation; SUR: surgery; RT: radiotherapy; BT: brachytherapy; HT: hyperthermia, CH: chemotherapy. Interval P-R: interval between primary tumor and (first) recurrence or metastatic disease (in months). n.a.: not applicable. Prior treatments: other treatment for recurrent, metastatic, or advanced disease, different from the primary treatment and CarboTaxol. Interval CH-vacc: interval between the starting date of the 2nd cycle of CarboTaxol and the date of vaccination with HPV16-SLP. Interval vacc-CH: interval between the date of vaccination and the date of the 3rd cycle (or 4th in case of patient ID6008 §) of chemotherapy with CarboTaxol.

Table s2 Adverse events systemically and at vaccination site. Systemic adverse events (AE) observed in the 12 patients in cohort 2, which might be vaccine-related and are defined as definite, probable, or possible. Local adverse events (AE at injection site) are shown for all 12 patients in cohort 2 who received the single HPV16-SLP vaccination. Shown are the number (N) and the percentage (%) of a total of 12 patients. Injection site AEs were scored at 15 minutes, 1 and 4 hours, 3 weeks, and at regular visits > 6 weeks after vaccination. * Long-term follow-up (> 6 weeks) could not be established for one patient who was deceased (N = 11 at > 6 weeks). Total reflects the maximal injection site reaction for each patient as determined for the single vaccination consisting of an injection of a mix of E6 peptides and a mix of E6/E7 peptides in two separated sites.

Systemically	< 24h	> 24h; < 3 wks	Vaccine related	Remark
Fever	1		definite	
Fever		2	possible	
Myalgia		1	possible	
Nausea		1	possible	
Vomiting		1	possible	
Painfull extremities		1	probable	
Stitch abcess		1	possible	1 wk after vaccination
Nefrodrain infection		1	possible	2 wks after vaccination

Locally (Injection sites)	Time after vaccination					Total
	15 min	1 hour	4 hours	3 weeks	>6 weeks*	
SWELLING						
0	2 (17%)	0 (0%)	1 (8%)	3 (25%)	3 (27%)	0 (0%)
< 5	9 (75%)	9 (75%)	9 (75%)	4 (33%)	7 (64%)	5 (42%)
5-10	1 (8%)	3 (25%)	2 (17%)	5 (42%)	1 (9%)	7 (58%)
>10	0 (0%)	0 (0%)	0 (0%)	0 (0%)	0 (0%)	0 (0%)
ERYTHEMA						
none	3 (25%)	2 (17%)	4 (33%)	6 (50%)	7 (64%)	1 (8%)
mild	9 (75%)	10 (83%)	7 (58%)	4 (33%)	3 (27%)	8 (67%)
moderate	0 (0%)	0 (0%)	1 (8%)	2 (17%)	0 (0%)	2 (17%)
severe	0 (0%)	0 (0%)	0 (0%)	0 (0%)	1 (9%)	1 (8%)
TEMPERATURE						
none	2 (17%)	1 (8%)	4 (33%)	4 (33%)	10 (91%)	0 (0%)
mild	10 (83%)	11 (93%)	8 (67%)	7 (58%)	1 (9%)	11 (92%)
moderate	0 (0%)	0 (0%)	0 (0%)	1 (8%)	0 (0%)	1 (8%)
severe	0 (0%)	0 (0%)	0 (0%)	0 (0%)	0 (0%)	0 (0%)
PAIN						
none	9 (75%)	10 (83%)	9 (75%)	6 (50%)	7 (64%)	6 (50%)
mild	1 (8%)	2 (17%)	3 (25%)	5 (42%)	4 (36%)	3 (25%)
moderate	2 (17%)	0 (0%)	0 (0%)	0 (0%)	0 (0%)	2 (17%)
severe	0 (0%)	0 (0%)	0 (0%)	1 (8%)	0 (0%)	1 (8%)
ITCH						
none	12 (100%)	12 (100%)	10 (83%)	7 (58%)	11 (100%)	6 (50%)
mild	0 (0%)	0 (0%)	2 (17%)	5 (42%)	0 (0%)	6 (50%)
moderate	0 (0%)	0 (0%)	0 (0%)	0 (0%)	0 (0%)	0 (0%)
severe	0 (0%)	0 (0%)	0 (0%)	0 (0%)	0 (0%)	0 (0%)
ULCERATION					1 (9%)	1 (8%)
CTCEA	Administered SLP:		E6	E6/E7		
grade 1			5 (42%)	6 (50%)		
grade 2			6 (50%)	6 (50%)		
grade 3			1 (8%)	0 (0%)		

CTCEA: common terminology criteria for adverse events

Figure s1 T-cells are not affected by CarboTaxol treatment. Wild-type *C57BL/6* mice were injected on day 0 with 1×10^5 TC-1 tumor cells. Eight days later, when tumors were palpable, mice were treated systemically with carboplatin (day 8) and paclitaxel (day 8 and 9) with or without addition of synthetic long HPV16 E7₄₃₋₇₇ peptide in Montanide in the opposite flank. Chemotherapy treatment was repeated one week after initial treatment, and vaccination was boosted 14 days after initial treatment. Shown is the quantification of the percentage of (A) CD4⁺ T-cells, (B) CD8⁺ T-cells, and (C) vaccine-specific cells within the CD8⁺ population as determined by H2-Db E7₄₉₋₅₇ (RAHYNIVTF) tetramer staining. Column 1 vs 7 ($p = 0.008$); column 2 vs 7 ($p = 0.007$), column 3 vs 7 ($p = 0.009$), column 4 vs 7 ($p = 0.007$). $N = 8$ mice in the tumor-bearing groups, $N = 4$ in the naïve group, data are representative of two individual experiments and expressed as mean plus SEM. Data were analyzed by one-way ANOVA followed by Tukey's post-hoc analysis.

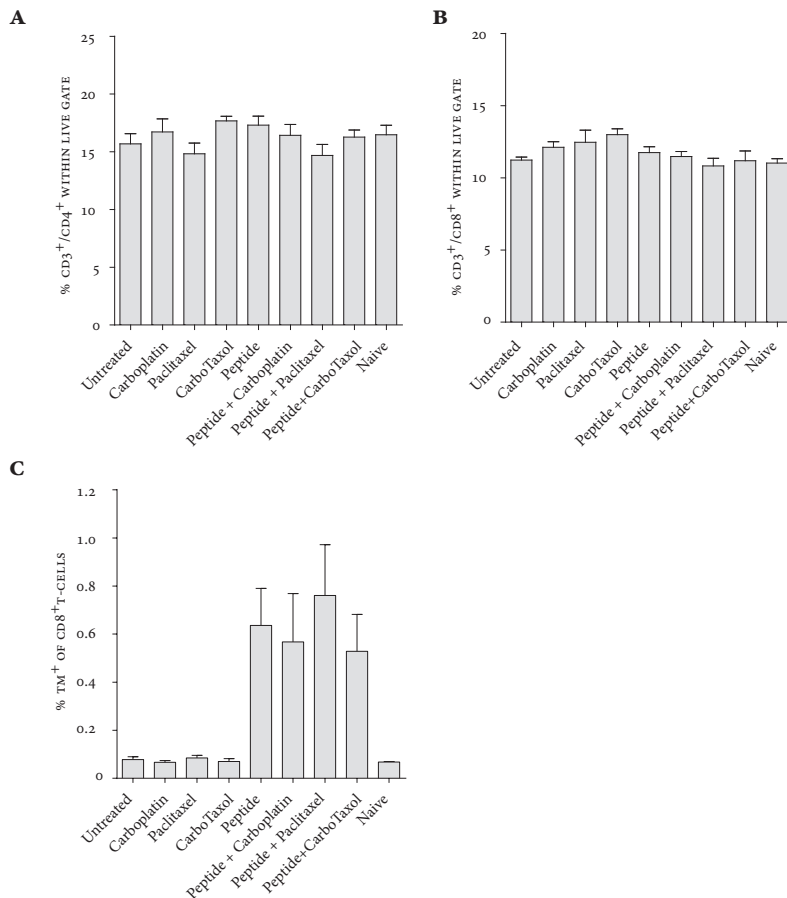


Figure S2 The delay in tumor growth does not differ between the treatment groups. Wild-type c57BL/6 mice were injected with TC-1 tumor cells. Eight days later, when tumors were palpable, mice were treated with synthetic long HPV16 E7₄₃₋₇₇ peptide in Montanide in the opposite flank. Carboplatin was administered on day 14, paclitaxel on day 14 and 15. Tumor size was measured over time and shown as the mean tumor size measured two-dimensionally (mm²) plus SEM. The significance of differences in tumor size was calculated for day 18 using one-way ANOVA. The tumor size in the untreated group of mice was significantly different from that of the peptide-treated mice ($p = 0.0003$), the CarboTaxol-treated mice ($p = 0.01$), and the peptide plus CarboTaxol treated group ($p < 0.0001$), whereas there was no significant difference between the different treatment groups. Experiment was performed with 5-7 mice per group; data shown are representative of two individual experiments.

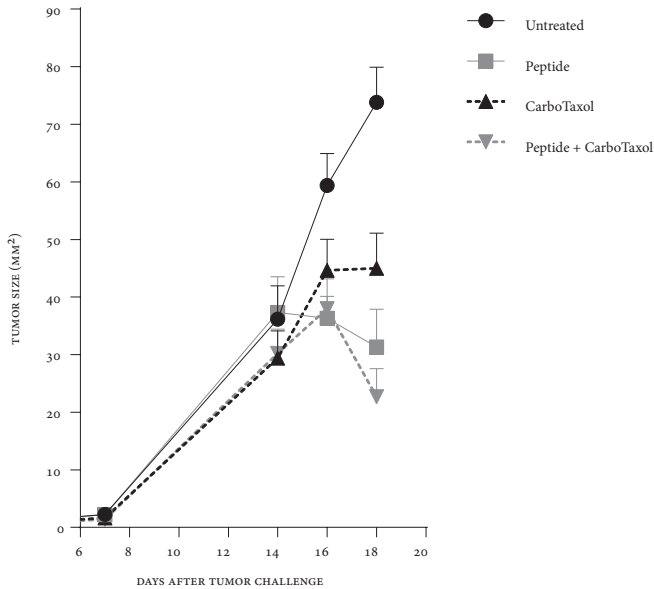


Figure s3 Chemotherapy does not hamper T-cells but decreases myeloid cell frequencies.

Wild-type C57BL/6 mice were injected with TC-1 tumor cells. (A) As the tumors grew if left untreated, the frequency of myeloid cells increased and the percentage of T-cells decreased as measured in the blood of the tumor-bearing mice. In another experiment, TC-1 tumor cells were injected. Eight days later, when tumors were palpable, mice were treated with synthetic long HPV16 E743-77 peptide in Montanide in the opposite flank. Carboplatin was administered on day 14, paclitaxel on day 14 and 15. Flow cytometry was used to quantify the percentage (mean plus SEM) of (B) CD4⁺ T-cells (Column 1 vs 4 (p = 0.001) and 5 (p = 0.008); column 4 vs 2 (p = 0.01) and 3 (p = 0.04), (C) CD8⁺ T-cells, (D) the vaccine-specific cells within the CD8⁺ T-cell population [Column 3 vs 1 (p = 0.02), 2 (p = 0.003) and 4 (p = 0.004)], (E) monocytes, which were identified as F4/80 and CD11b positive [Column 4 vs 2 (p = 0.049) and 3 (p = 0.03)], and (F) dendritic cells [Column 4 vs 1 (p = 0.002), 2 (p = 0.005), 3 (p = 0.0008) and 5 (p = 0.02)]. (G) Overlay of F4/80⁺ and F4/80⁻ cells in flow cytometry plots that show Gr-1 and CD11b expression of all live cells in the blood of treated mice. (H) Flow cytometry plots representing CD11c and CD11b expression of all live cells in the blood of treated mice. The experiment was performed with 5-7 mice per group, and data shown are representative of two individual experiments. Data were analyzed by one-way ANOVA followed by Tukey's post-hoc analysis.

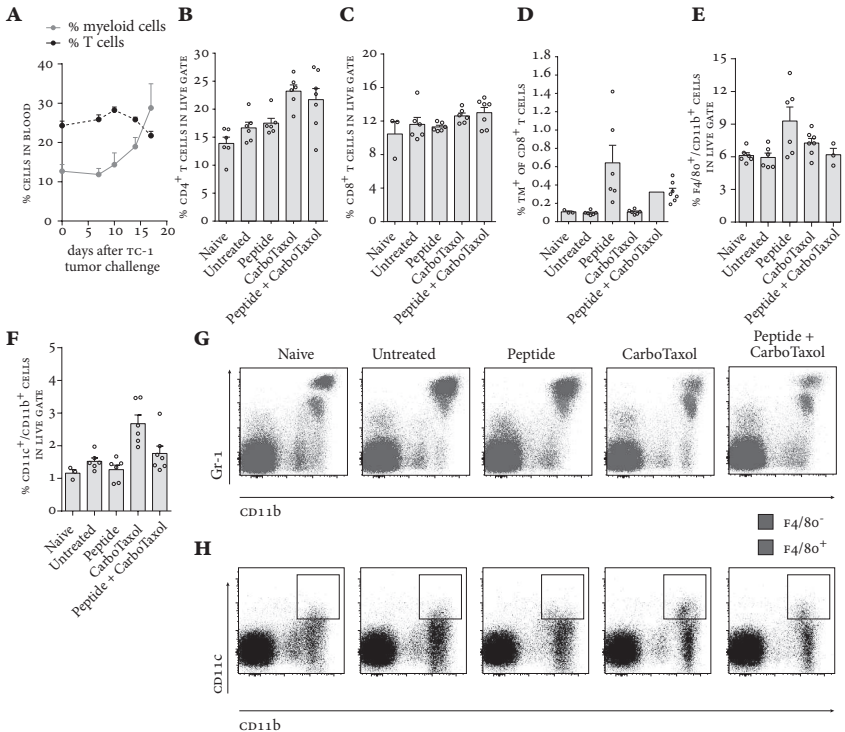


Figure s4 The combination of carboplatin and paclitaxel results in the strongest reduction of circulating myeloid cells. Wild-type *c57BL/6* mice were injected with TC-1 tumor cells. Carboplatin was administered on day 14 and paclitaxel on day 15. Flow cytometry was used to quantify the percentage of CD11b^{hi} cells in the blood. The experiment was performed with 5 mice per group. Data (shown as mean plus SEM) were analyzed by one-way ANOVA followed by Tukey's post-hoc analysis.

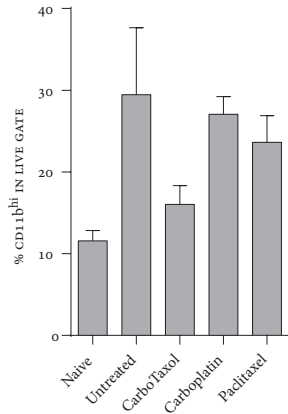


Figure s5 CarboTaxol therapy does not influence general immune parameters. Blood samples obtained at different time points (before, during, and after chemotherapy) from 5 of the 6 cervical cancer patients in cohort 1 were subjected to flow cytometry to determine the frequency of (A) CD4⁺ and (B) CD8⁺ T-cells. Plotted are the percentages of these two types of T-cells within the lymphocyte gate. PBMC samples from (C) 5 of the 6 patients in cohort 1 and (D) the 12 patients in cohort 2 were stimulated with PHA to test their capacity to proliferate. The results are depicted as stimulation index. (E) The quality of the antigen presenting cells in the patients' PBMCs from cohort 2 was analyzed by mixed lymphocyte reaction. The proliferative capacity of third party PBMC is depicted as stimulation index. Data (shown as median plus interquartile range) were analyzed by repeated measures model.

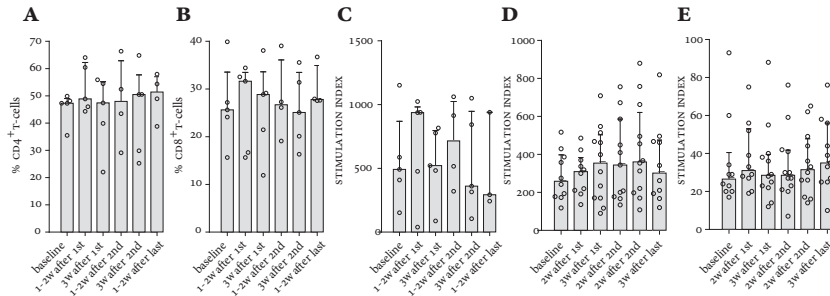


Figure s6 CarboTaxol therapy alters the relative frequencies of myeloid cells and lymphocytes. (A) The myeloid cells and lymphocytes as percentage of CD45⁺ cells are depicted for healthy donors (HD, N = 19) and cervical cancer patients (P, N = 18) at baseline. Column 1 vs 2 (p < 0.0001); column 3 vs 4 (p < 0.0001). The shifts in the frequency of (B) myeloid cells [Column 1 vs 2 (p=0.04), 3 (p = 0.007), 4 and 5 (p = 0.004)] and (C) lymphocytes [Column 1 vs 2 (p = 0.02), 3 (p = 0.0009), 4 and 5 (p = 0.0002)] compared to baseline values are depicted for the blood samples obtained from the cervical cancer patients of cohort 2 before, during, and after the last cycle of chemotherapy with CarboTaxol. Data (shown as median plus interquartile range) were analyzed by repeated measures model.

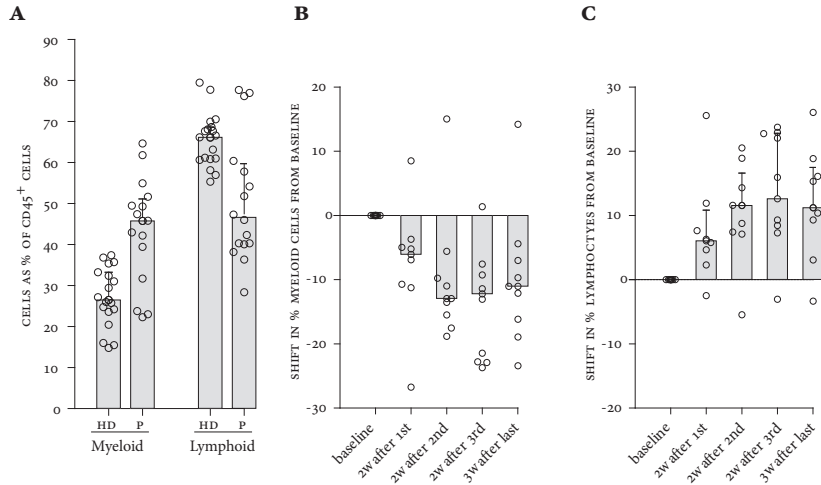


Figure s7 Flow cytometric analysis of myeloid cells and T-cells in blood samples of cervical cancer patients. Blood samples of the cervical cancer patients are stained with three different sets of antibodies and acquired by flow cytometry to determine the composition of immune cells within the sample and over time within an individual patient. An example of the gating strategy is shown for these three sets of antibodies. (A) In the macrophage-like set, first the single cells were gated, then the CD45⁺ cells followed by the selection of non T and non B cells (CD3⁻CD19⁻). Then, the HLA-DR⁺CD11a⁻ cells were selected. Next, this myeloid cell population was plotted for the expression of CD14 and CD11b, revealing 5 subpopulations. Each of these subpopulations was then analyzed for the expression of CD11c, CD16, CD206, and CD163.

A

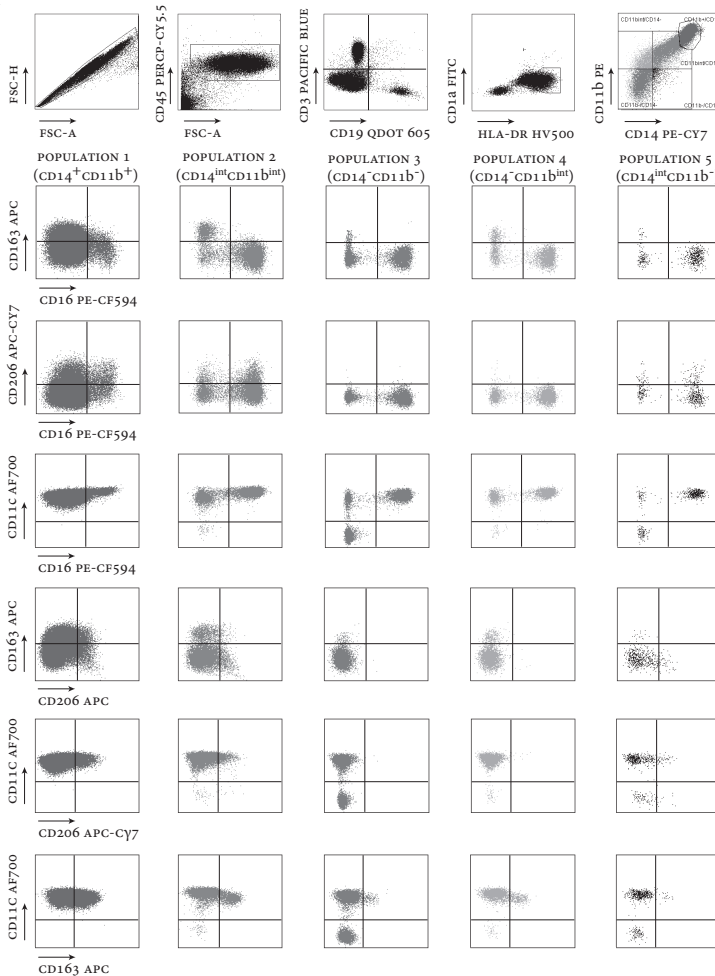


Figure s7(B) In the myeloid-derived suppressor cell (MDSC) set, we used the same strategy as in the macrophage panel for the first three plots. Then, the HLA-DR^{low} subpopulation within the myeloid cells (CD3⁺CD19⁻) was selected and the expression of CD14 (for myeloid MDSC; mMDC) and CD15 (for granulocytic MDSC; gMDSC) plotted. Both subsets of MDSC as well as the double negative cells (CD14⁻CD15⁻) were analyzed for the expression of the other markers: CD11b, CD33, CD34, and CD124.

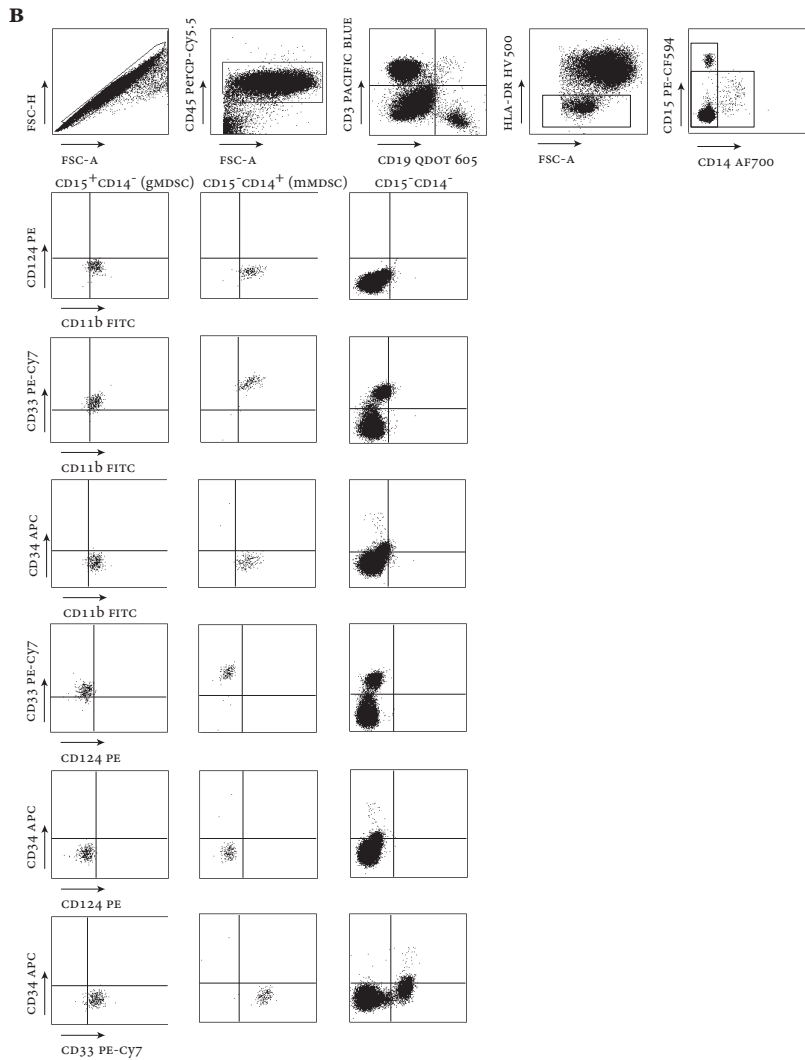


Figure s7(c) In the inhibitory receptors set, the CD3⁺ cells were selected from the single cells, followed by the live gate. Then, CD4 was plotted versus CD8 and within each of these two T-cell populations, the expression of TIM-3, PD-1, and CTLA-4 was determined.

C

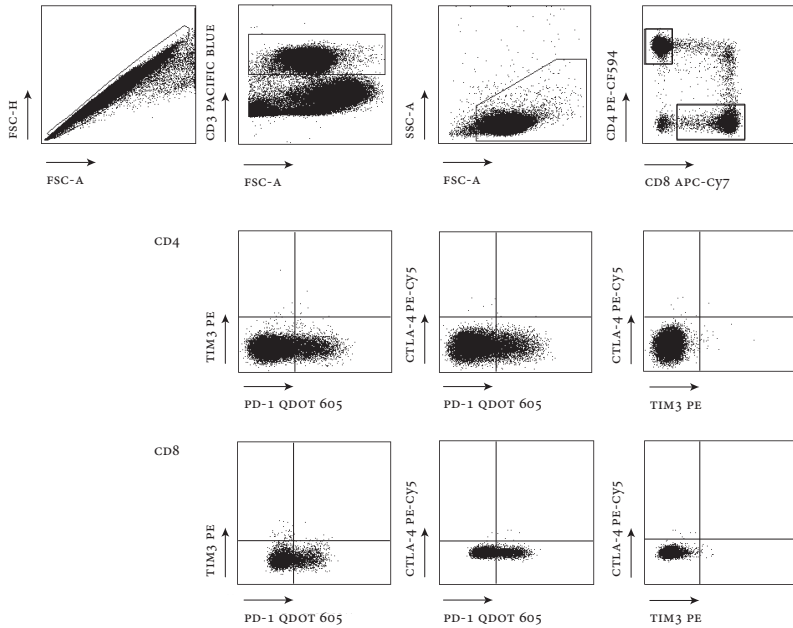


Figure s8 CarboTaxol treatment affects different subpopulations of CD11b and/or CD14 positive myeloid cells. The phenotypic analysis of the blood samples of cervical cancer patients was performed with the macrophage antibody set and using the gating strategy shown in fig. S7A, for the 5 different populations which could be defined within the CD45⁺CD3⁻CD19⁻CD11a⁻HLA-DR⁺ subpopulation of cells on the basis of differential expression of the markers CD14 and CD11b. These subsets of cells were followed over time in all 12 vaccinated patients of cohort 2 and are plotted as median plus interquartile range. **(A)** Population 2, with intermediate expression of both CD14 and CD11b. Column 1 vs 2 ($p = 0.005$), 3 ($p = 0.03$), 4 ($p = 0.01$) and 6 ($p = 0.004$). **(B)** Population 3, lacking the expression of both markers. Column 1 vs 3 to 6 ($p < 0.0001$). Column 2 vs 3 and 6 ($p = 0.04$), 4 ($p = 0.004$). **(C)** Population 4, with intermediate CD11b expression and no CD14. Column 1 vs 6 ($p = 0.03$). **(D)** Population 5, with intermediate CD14 expression and no CD11b. Column 1 vs 4 ($p = 0.008$). Column 2 vs 3 and 6 ($p = 0.02$), and 4 ($p = 0.002$). Data (shown as median plus interquartile range) were analyzed by repeated measures model.

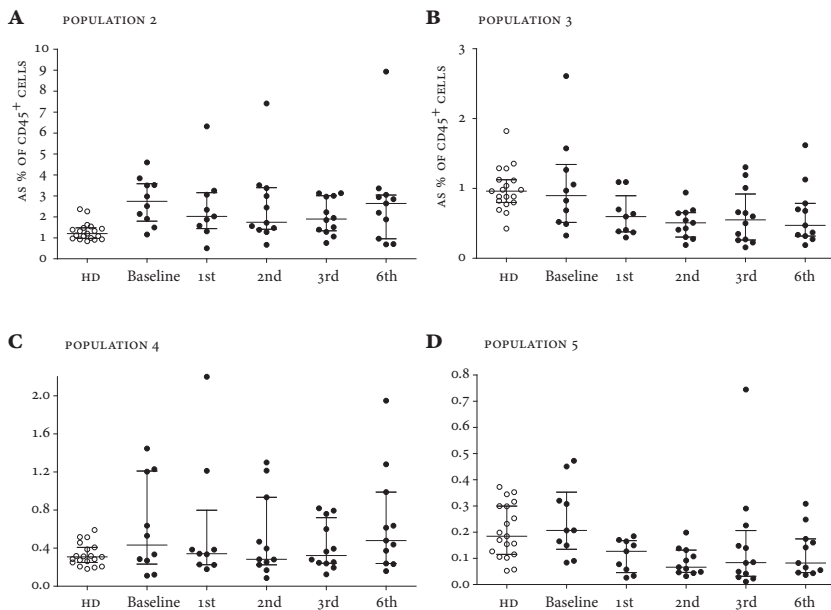


Figure s9 CarboTaxol therapy reduces the number of regulatory T-cells in cervical cancer patients. The T-cells in the blood samples of cervical cancer patients of cohort 2 as well as from healthy donors (HD) were stained for multiple markers indicative of inhibitory receptors. The frequency is depicted as percentage of the CD45⁺ cells. (A) CD4⁺ T-cells [Column 1 vs 2 (p = 0.009)]. (B) CD8⁺ T-cells. (C) The frequency within the CD4⁺ T-cells was calculated as a percentage of CD45⁺ cells that express TIM3 alone [left; column 1 vs 2 (p = 0.01); column 2 vs 4 (p = 0.002), 5, and 6 (p = 0.01)], both TIM3 and PD-1 [middle; column 1 vs 2 (p = 0.007), 3 (p = 0.01), 4 (p = 0.04), and 5 (p = 0.004)], or PD-1 alone [right; column 1 vs 2 (p = 0.0008), 3 (p = 0.001), 4 (p = 0.0001), 5 (p < 0.0001), and 6 (p = 0.002)]. (D) The frequency within the CD8⁺ T-cells calculated as percentage of CD45⁺ cells that express TIM3 alone [left; column 1 vs 2 (p = 0.01), 3 (p = 0.004), 4 (p = 0.02), 5 (p = 0.004), and 6 (p = 0.009)], both TIM3 and PD-1 [middle; column 1 vs 2 (p = 0.008), 3 (p = 0.01), 5 (p = 0.03)], or PD-1 alone [right; column 1 vs 2 (p = 0.04)]. (E) Measurement of regulatory T-cells within the CD3⁺CD8⁺CD4⁺ population by expression of CD25⁺, CD127⁻, and Foxp3⁺ (Column 1 vs 2 and 3 (p < 0.0001), 4 (p = 0.001), and 5 (p = 0.002); column 2 vs 4 (p = 0.007) and 5 (p = 0.005). Data (shown as median plus interquartile range) were analyzed by repeated measures model.

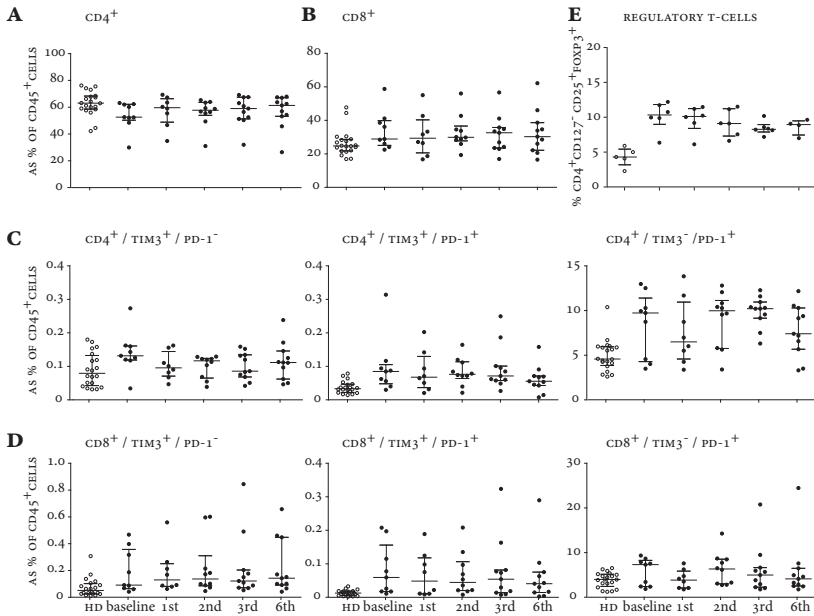


Figure S10 HPV16-SLP vaccination induces poly-functional T-cells. An in depth analysis by intracellular cytokine staining could be performed to determine the cytokine production specifically upon recognition of HPV16 E6 and/or E7 peptides for 6 patients in the second cohort. The stacked bars show the frequency of CD4⁺ T-cells producing only TNFα (TNFα⁺ IL-2⁻ IFNγ⁻; white bars), both TNFα and IL-2 (TNFα⁺ IL-2⁺ IFNγ⁻; gray bars), and all three cytokines (TNFα⁺ IL-2⁺ IFNγ⁺; black bars) for the two viral oncoproteins in the indicated blood samples.

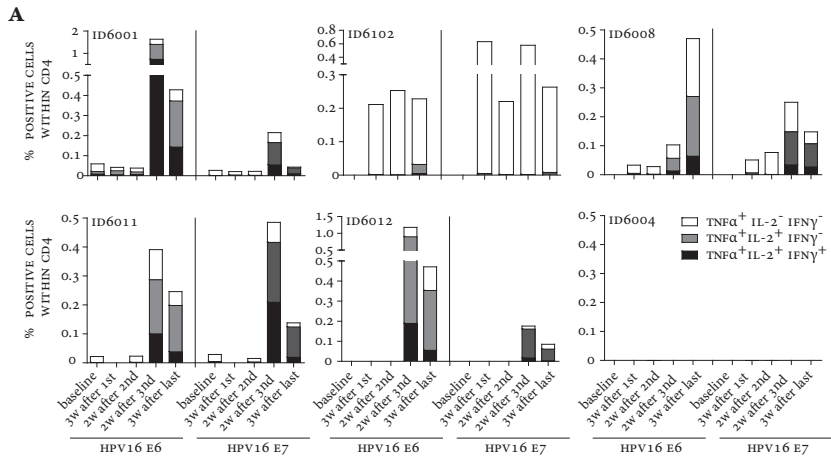


Figure S11 The vaccine-induced HPV16-specific T-cell response is stronger in patients vaccinated during chemotherapy. The median stimulation index (plus interquartile range) of the 6 tested peptide pools per patient was calculated for all patients at each indicated time point and depicted for (A) recurrent cervical cancer patients in the previously conducted clinical trial¹⁵, in which the patients received HPV16-SLP vaccination at least one month after they had undergone chemotherapy and (B) advanced cervical cancer patients who were vaccinated during chemotherapy as described in the current trial. The blood samples were taken before vaccination (pre-vac), or after 1 (1-vac), 2 (2-vac), or 4 (4-vac) vaccinations as indicated. FU, follow-up blood sample taken after the last cycle of chemotherapy. In both graphs, the pre-vaccinated median stimulation index is significantly different from the two post-vaccinated responses ($p < 0.0001$). Data were analyzed by paired T-test.

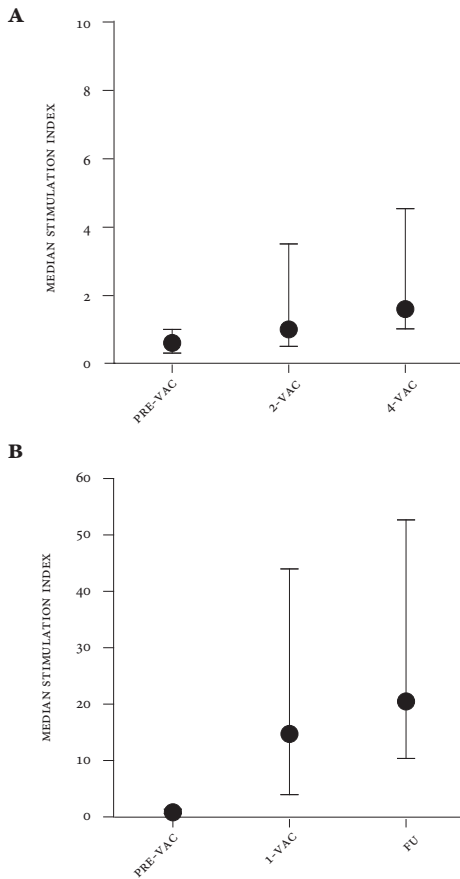


Figure S12 Myeloid cell depletion improves the response of PBMC to stimulation in vitro. The CD14⁺ myeloid cells were depleted in the pre-chemotherapy PBMC samples of two advanced cervical cancer patients via magnetic cell sorting. The depleted and non-depleted PBMCs were stimulated with autologous monocytes, which were pulsed with a mix of recall antigens (FLU and MRM), a pool of HPV16 E6 and E7 SLP, or a pool of p53 SLP, for 11 days after which the bulk culture was tested in a 3-day proliferation assay. At the top, the forward (FSC) and side (SSC) scatter plots are shown for both the non-depleted and depleted PBMC. The percentages indicate the frequencies of lymphoid and myeloid cells. In the FSC and CD14 plots (bottom), the CD14⁺ cell frequencies in PBMC before and after the CD14 depletion are shown. On the right, the graphs display the antigen-specific proliferation (in counts per minute, cpm, shown as mean of triplicate wells plus standard deviation) for the three different bulk cultures after stimulation with non-pulsed (peptide -) or antigen-pulsed (peptide +) autologous monocytes

